

A NUMERICAL STUDY ON RESPONSE FACTORS FOR
STEEL PLATE SHEAR WALL SYSTEMS

A THESIS SUBMITTED TO
THE GRADUATE SCHOOL OF NATURAL AND APPLIED SCIENCES
OF
MIDDLE EAST TECHNICAL UNIVERSITY

BY

CAN OZAN KURBAN

IN PARTIAL FULFILLMENT OF THE REQUIREMENTS
FOR
THE DEGREE OF MASTER OF SCIENCE
IN
CIVIL ENGINEERING

JULY 2009

Approval of the thesis:

**A NUMERICAL STUDY ON RESPONSE FACTORS FOR
STEEL PLATE SHEAR WALL SYSTEMS**

submitted by **CAN OZAN KURBAN** in partial fulfillment of the requirements for
the degree of **Master of Science in Civil Engineering Department, Middle East
Technical University** by,

Prof. Dr. Canan Özgen
Dean, Graduate School of **Natural and Applied Sciences**

Prof. Dr. Güney Özcebe
Head of Department, **Civil Engineering**

Assoc. Prof. Dr. Cem Topkaya
Supervisor, **Civil Engineering Dept., METU**

Examining Committee Members:

Assoc. Prof. Dr. Ahmet Yakut
Civil Engineering Dept., METU

Assoc. Prof. Dr. Cem Topkaya
Civil Engineering Dept., METU

Assoc. Prof. Dr. Altuğ Erberik
Civil Engineering Dept., METU

Asst. Prof. Dr. Ayşegül Askan Gündoğan
Civil Engineering Dept., METU

Volkan Aydoğan
Civil Engineer (M.S.), PROMA

Date: 06.07.2009

I hereby declare that all information in this document has been obtained and presented in accordance with academic rules and ethical conduct. I also declare that, as required by these rules and conduct, I have fully cited and referenced all material and results that are not original to this work.

Name, Last name: Can Ozan Kurban

Signature :

ABSTRACT

A NUMERICAL STUDY ON RESPONSE FACTORS FOR STEEL PLATE SHEAR WALL SYSTEMS

Kurban, Can Ozan

M.Sc., Department of Civil Engineering

Supervisor: Assoc. Prof. Dr. Cem Topkaya

July 2009, 53 pages

Design recommendations for steel plate shear wall (SPSW) systems have recently been introduced into seismic provisions for steel buildings. Response modification, overstrength, and displacement amplification factors for SPSW systems presented in the design codes were based on professional experience and judgment. A numerical study has been undertaken to evaluate these factors for SPSW systems. Forty four unstiffened SPSWs possessing different geometrical characteristics were designed based on the recommendations given in the AISC Seismic Provisions. Bay width, number of stories, story mass, and steel plate thickness were considered as the prime variables that influence the response. Twenty records were selected to include the variability in ground motion characteristics. In order to provide a detailed analysis of the post-buckling response, three-dimensional finite element analyses were conducted for the 44 structures subjected to the selected suite of earthquake records. For each structure and earthquake record two analyses were conducted in which the first one includes geometrical nonlinearities and the other one includes both geometrical and material nonlinearities, resulting in a total of 1760 time history analysis. In this thesis, the details of the design and analysis methodology are given. Based on the analysis results response modification, overstrength and displacement amplification factors for SPSW systems are evaluated.

Keywords: Steel plate shear wall, finite element, response modification, overstrength, displacement amplification.

ÖZ

ÇELİK PLAKALI PERDE DUVAR SİSTEMLERİN DAVRANIŞ KATSAYISILARININ NÜMERİK OLARAK İNCELENMESİ

Kurban, Can Ozan

Yüksek Lisans, İnşaat Mühendisliği Bölümü

Tez Yöneticisi: Doç. Dr. Cem Topkaya

Temmuz 2009, 53 sayfa

Deprem şartnamelerinde çelik plakalı perde duvarlarla ilgili tasarım kurallarına yeni yeni yer verilmeye başlanmıştır. Şartnamelerde, çelik plakalı perde duvar sistemler için taşıyıcı sistem davranış katsayısı, dayanım fazlalığı ve deplasman büyütme katsayılarına ilişkin bazı değerler yer almaktadır, fakat bu değerler çoğunlukla mühendislik deneyimine dayalıdır. Bahsedilen katsayıların tayini için parametrik bir çalışma yapılmıştır. Öncelikle, farklı geometrik özelliklere sahip 44 tane çelik plakalı perde duvar sistemli yapı, AISC Deprem Yönetmeliği'ne göre tasarlanmıştır. Parametrik çalışmada değişken olarak, plaka kalınlığı, plaka görünüm oranı (en-boy oranı), kat sayısı ve kat kütlesi alınmıştır. Parametrik çalışma için yer hareketlerinin özelliklerinde değişiklikler olması açısından 20 farklı yer hareketi seçilmiştir. Burkulma sonrası davranışı gözlemlemek amacıyla çelik plakalı perde duvar sistemler 3 boyutlu sonlu elemanlar metodu kullanılarak modellenmiş ve 44 yapının herbirinin davranışı, seçilen 20 adet yer hareketi altında incelenmiştir. Her yapı ve yer hareketi için iki tür analiz yapılmıştır. İlkinde sadece geometrik düzensizliklere, ikincisinde ise hem geometrik düzensizliklere hem de malzeme düzensizliklerine yer verilmiştir. Böylelikle, toplam 1760 adet zaman tanım alanı analizi yapılmıştır. Bu tezde, çelik plakalı perde duvarların tasarım ve analizlerinin detaylarından bahsedilmiştir. Çelik

plakalı perde duvarların taşıyıcı sistem davranış katsayısı, dayanım fazlalığı ve deplasman büyütme katsayıları, analiz sonuçlarına göre irdelenmiştir.

Anahtar Kelimeler: Çelik plakalı perde duvar, sonlu elemanlar metodu, taşıyıcı sistem davranış katsayısı, dayanım fazlalığı, deplasman büyütme.

To my family...

ACKNOWLEDGMENTS

I would like to express very special thanks to my supervisor Assoc. Prof. Dr. Cem Topkaya for his guidance, support, advice and patience during this study.

I wish to express my respect and appreciation to my bosses Mr. Utku Özyurt and Mr. Taylan Özgünlü for their endless patience and tolerance throughout the research.

Anıl Ercan deserves my grateful thanks for motivating, supporting and helping me to complete this study as she does in all parts of my life.

Special thanks go to my colleagues and my friends, especially Ahmet Kuşyılmaz, Özgür Erdoğan, Özkan Kale and Sertaç Küçükarslan, for their criticism on the study and contribution to my educational and professional life.

Finally, I wish to present my special thanks to my mother F. Hülya Kurban and my father Salih Kurban for their unlimited patience and support during my whole life.

This study was supported by a contract from The Scientific & Technological Research Council of Turkey (TÜBİTAK – 105M242). Also, the scholarship provided by TÜBİTAK during my graduate study is highly acknowledged.

TABLE OF CONTENTS

ABSTRACT.....	iv
ÖZ.....	vi
ACKNOWLEDGMENTS.....	ix
TABLE OF CONTENTS.....	x
LIST OF TABLES.....	xii
LIST OF FIGURES.....	xiii
CHAPTERS	
1.INTRODUCTION.....	1
1.1 Background.....	1
1.1.1 Background on Steel Plate Shear Walls.....	1
1.1.1.1 Applications of Steel Plate Shear Walls.....	4
1.1.2 Background on R , Ω_o , C_d Factors.....	10
1.2 Objective of the Study.....	12
2.NUMERICAL STUDY OF SPSW SYSTEMS.....	13
2.1 General.....	13
2.2 Design of SPSW Systems.....	18
2.3 Selection of a Suite of Ground Motions.....	23
2.4 Finite Element Modeling, Analysis and Verification.....	26
3.ANALYSIS RESULTS AND FINDINGS.....	31
3.1 Results of the Numerical Study.....	31
3.1.1 Overstrength Factor (Ω_o).....	35

3.1.2 Ductility Reduction Factor (R_{μ})	38
3.1.3 Response Modification Factor (R)	41
3.1.4 Displacement Amplification Factor (C_d)	43
4.LIMITATIONS, SUMMARY AND CONCLUSIONS OF THE STUDY	47
4.1 Limitations of the Study and Future Research Needs.....	47
4.2. Summary and Conclusions.....	48
REFERENCES.....	50

LIST OF TABLES

TABLES

Table 2.1 – SPSW Used in the Numerical Study.....	16
Table 2.2 – Details of Selected Ground Motion Records	24

LIST OF FIGURES

FIGURES

Figure 1.1 - A Typical Steel Plate Shear Wall	1
Figure 1.2 - (a) A Typical Plate Girder and (b) A SPSW system	2
Figure 1.3 - (a) A Standard SPSW system and (b) A Dual SPSW system	2
Figure 1.4 - Residential Building With SPSW System in Atherton, CA	5
Figure 1.5 - Residential Building With SPSW System in San Mateo County, CA	5
Figure 1.6 - US Federal Courthouse, Seattle	6
Figure 1.7 - Core Wall in the Middle of ING Building, Montreal, CANADA.....	7
Figure 1.8 - SPSW details for ICRM Building, Montreal, CANADA	7
Figure 1.9 - Kobe City Hall Building, Japan	8
Figure 1.10 - A 22 Story Building in Mexico with SPSW System.....	9
Figure 1.11 - General Structural Response	11
Figure 2.1 - Floor Plans.....	14
Figure 2.2 - Response Spectra for Selected Earthquake Records and Design Base Acceleration for SPSW	25
Figure 2.3 - (a) Shear Force – Displacement Response of a SPSW System From the Experiment Performed by Driver et al., 1998 (b) Shear Force – Displacement Response of the Same SPSW System from the Numerical Analysis Performed in This Study.....	27
Figure 2.4 - (a) A Typical Finite Element Mesh and (b) a Plot of von Mises Equivalent Plastic Strain	28
Figure 3.1 - (a) A Typical Elastic(a) and Inelastic(b) Base Shear Response for a Representative 6 Story SPSW.....	32
Figure 3.2 - Pushover Like Curve	34
Figure 3.3 - Ductility reduction Factor Against Structural Ductility.....	39

Figure 3.4 - Variation of Ductility Reduction Factor With Maximum Interstory Drift Ratio.....	40
Figure 3.5 - Variation of Response Modification Factor With Maximum Interstory Drift Ratio.....	42
Figure 3.6 -The Ratio of the Maximum Interstory Drift Obtained by Conducting Inelastic and Elastic Analysis Against the Fundamental Natural Period of the System.....	44
Figure 3.7 - Variation of Displacement Amplification Factor With Response Modification Factor.....	46

CHAPTER 1

INTRODUCTION

1.1 Background

1.1.1 Background on Steel Plate Shear Walls

Steel plate shear walls (SPSW) can be used as a lateral load resisting system for buildings. A typical SPSW (Fig. 1.1) consists of stiff horizontal and vertical boundary elements (HBE and VBE) and infill plates. The resulting system is a stiff cantilever wall which resembles a vertical plate girder (Fig.1.2).

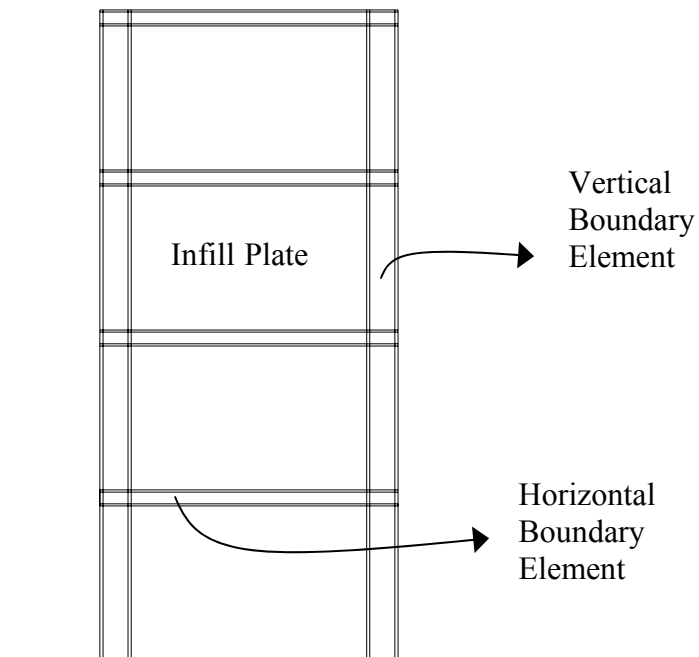


Figure 1.1 – A Typical Steel Plate Shear Wall

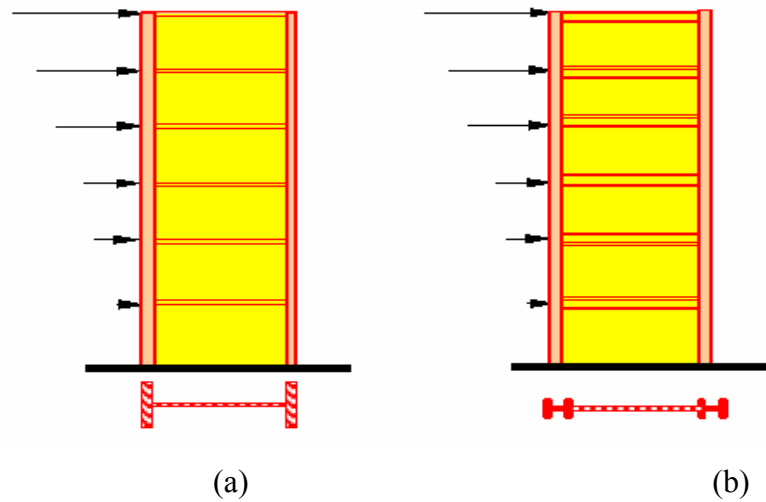


Figure 1.2 (a) A Typical Plate Girder and (b) A SPSW system [32]

There are two types of SPSW systems, which are the standard system and the dual system. In the standard system SPSW is used as the sole lateral load resisting system and pin type beam to column connections are used in the rest of the steel framing (Fig 1.3(a)). In the latter system, SPSW is a part of a lateral load resisting system and installed in a moment resisting frame. In this case forces are resisted by the frame and SPSW (Fig 1.3(b)). SPSW can have stiffened or unstiffened infill plates depending on the design philosophy.

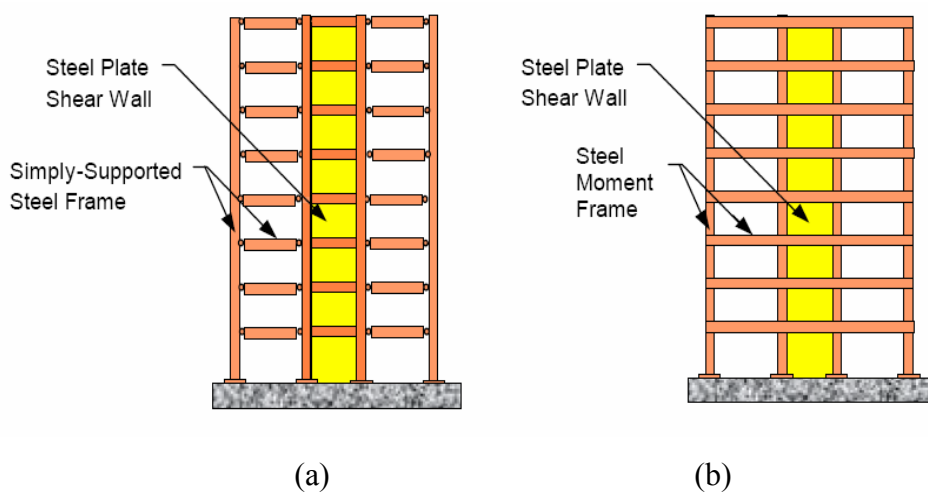


Figure 1.3 (a) A Standard SPSW system and (b) A Dual SPSW system [32]

Earlier designs used stiffeners to prevent buckling of infill plates under shear stresses. On the other hand, more recent approaches rely on post buckling strength. Based on the work of Wagner [31], it has been known that buckling does not necessarily represent the limit of structural usefulness and there is considerable post buckling strength possessed by restrained unstiffened thin plates. At the onset of buckling, which occurs at very low lateral loads, the load carrying mechanism changes from in-plane shear to an inclined tension field. The additional post buckling strength due to the formation of tension field can be utilized to resist lateral forces. Due to the cost associated with stiffeners most new designs employ unstiffened infill plates.

Design recommendations for SPSW systems are newly introduced into the AISC Seismic Provisions for Structural Steel Buildings [19]. These provisions basically present guidelines on the calculation of lateral load capacity of SPSW as well as recommendations on the seismic characteristics. Lateral load resisting capacity of SPSW systems has been studied experimentally and numerically in the past [1-16] and procedures for computing the nominal capacity are developed [16]. These experimental and analytical studies led to the development of code provisions. On the other hand, little is known on the seismic response characteristics of SPSW systems. Response modification (R), overstrength (Ω_o) and displacement amplification (C_d) factors have paramount importance in force-based seismic design procedures [17]. The amount of lateral forces and inelastic displacements and design of special elements such as the vertical boundary members are directly influenced by these factors. There are values presented in the AISC Seismic Provisions [19], however, these mostly depend on engineering judgment and on some observations during experiments and past earthquakes. Clearly there is a need for detailed investigation of these factors.

1.1.1.1 Applications of Steel Plate Shear Walls

SPSW systems have been used in numerous buildings, in the countries such as, the United States, Canada, Mexico, and Japan. Building types cover a wide range from single-family residential buildings to high-rise construction. Steel web plates have been used not only in new construction but also to retrofit existing buildings [23].

SPSW systems may be used in the buildings wherever the building function permits walls of moderate length. High-rise and mid-rise buildings, particularly having continuous building core and repetitive floor plans are well suited for SPSW [23].

Since 1970's, stiffened SPSW systems were used in the United States in new construction and also for seismic retrofitting of the existing buildings. In 1980's and 1990's, unstiffened SPSW systems were used in buildings in the United States [32].

In the United States, for a 1579 m² residence in Atherton, California the SPSW system was used in the buildings in which the VBEs are 76.2 centimeters center-to-center (Fig 1.4). Moreover, SPSW system was used for a 836 m² residence in San Mateo County to meet the owner's requirements according to which no important damage in the structural system be occurred in a probable earthquake (Fig 1.5). SPSW system was also used in the narrow North-South direction of the building core for the U.S. Federal Courthouse, which is a 23 story building in Seattle (Fig 1.6) [23].



Figure 1.4 – Residential Building With SPSW System in Atherton, CA [23]



Figure 1.5 – Residential Building With SPSW System in San Mateo County, CA
[23]



Figure 1.6 – US Federal Courthouse, Seattle [23]

Unstiffened steel plate shear wall systems have been constructed in Canada since the early 1980s. Canadian research is focused on unstiffened SPSW systems. For instance, a SPSW system was selected for the seven-story ING building in Ste-Hyacinthe, Quebec, due to a faster construction and gain of floor space, compared to the other structural systems (reinforced concrete walls and steel braced frames, etc). The design concept was based on a core of walls in the middle of the building (Figure 1.7). SPSW system was also used for additional two stories to an existing single-story building of the Institut de Recherches Cliniques de Montreal (ICRM) (Figure 1.8) [23].



Figure 1.7 – Core Wall in the Middle of ING Building, Montreal, CANADA [23]

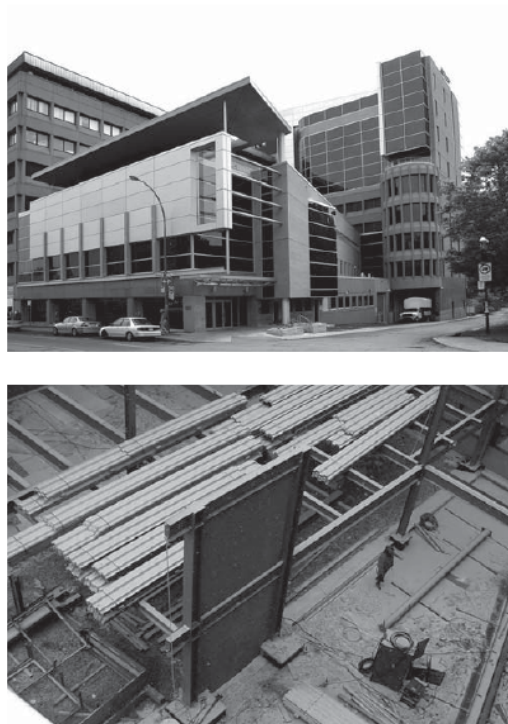


Figure 1.8 – SPSW details for ICRM Building, Montreal, CANADA [23]

In 1970's, stiffened SPSW systems were used in Japan in new construction and since that time buildings with SPSW systems have been constructed in Japan [32].

35-story Kobe City Hall Building, in Japan, is one of the most important buildings with SPSW systems in a highly seismic area (Fig 1.9). It was constructed in 1988 and was subjected to the 1995 Kobe earthquake, and received minor damages. The structural system in the building is a dual system (steel moment frames and SPSW together). In the three basement levels the shear walls are reinforced concrete. Composite walls were used in the first and second floors. Above the 2nd floor stiffened SPSW system was used [32].

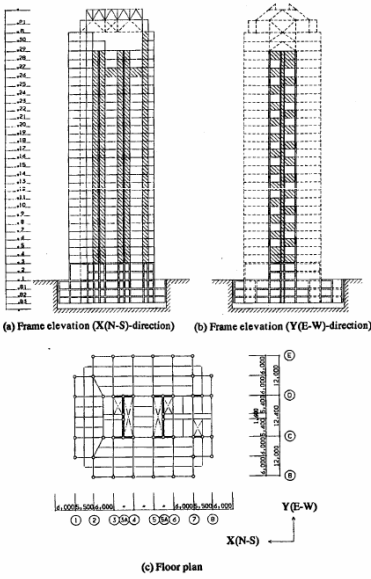


Figure 1.9 – Kobe City Hall Building, Japan [23]

In Mexico, a 22-story condominium building located on a hillside was firstly planned to be built as a reinforced concrete building with 3 m. story heights and a total height of 68.5 m (Fig 1.10). Nonetheless, a steel framing was also designed for cost comparison due to owners' request. The preliminary calculations revealed that the steel frames combined with the concrete shear walls around the elevator cores were more economical. Consequently, this structural system was selected for construction.

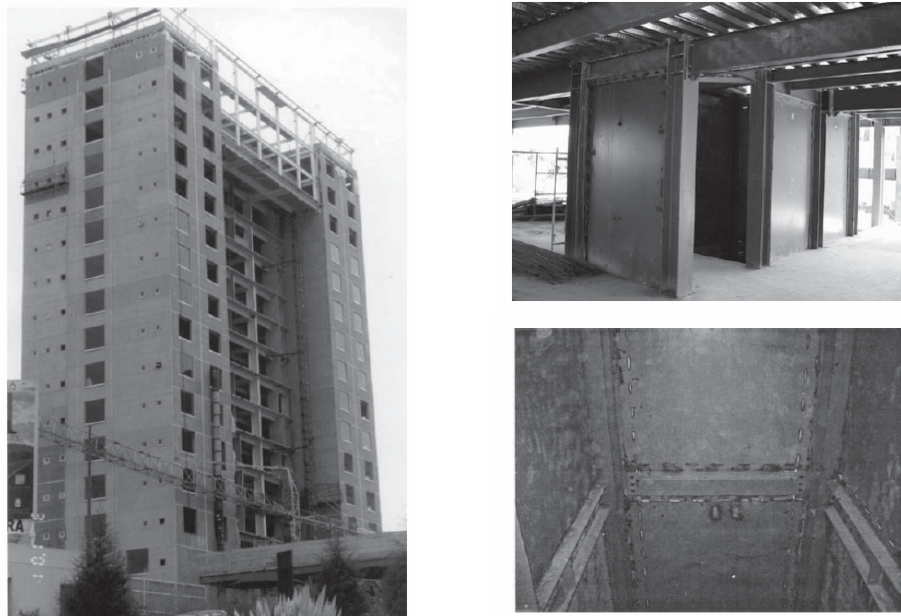


Figure 1.10 – A 22 Story Building in Mexico with SPSW System [23]

1.1.2 Background on R, Ω_o , C_d Factors

Response modification (R), overstrength (Ω_o) and displacement amplification (C_d) factors are used in force-based seismic design procedures [17]. An explicit formulation of these factors was proposed by Uang [18]. In this formulation, a typical global structural response shown in Fig. 1.11 is considered. In this figure, V_e is the ultimate elastic base shear, V_s is the base shear at first significant yield, V_y is the base shear at structural collapse level, Δ_s is the drift at first significant yield, Δ_y is the drift at structural collapse level, Δ_{\max} is the maximum amount of drift, μ_s is the ductility factor, Ω_o is the overstrength factor, R_μ is the ductility reduction factor, R is the response modification factor, and C_d is the displacement amplification factor. The following relationships hold [18]:

A properly designed structure usually provides certain amount of ductility and the structure can be designed economically to develop a maximum strength of V_y . The amount of ductility (μ_s) a structure experiences can be defined as:

$$\mu_s = \frac{\Delta_{\max}}{\Delta_y} \quad (1.1)$$

When the hysteretic energy dissipation due to the ductility of the system is considered, the elastic design force can be reduced to the yield strength level (V_y) by the ductility reduction factor R_μ :

$$R_\mu = \frac{V_e}{V_y} \quad (1.2)$$

The reserve strength that is present between the actual structural yield level (V_y) and the first significant yield level (V_s) is defined as the overstrength factor Ω_o :

$$\Omega_o = \frac{V_y}{V_s} \quad (1.3)$$

Displacement amplification factor (C_d) is the ratio between the Δ_{\max} and Δ_s , and is related to ductility and overstrength as follows:

$$C_d = \frac{\Delta_{\max}}{\Delta_s} = \mu_s \Omega_o \quad (1.4)$$

Response modification factor (R) which corresponds to the total force reduction can be derived as follows:

$$R = \frac{V_e}{V_s} = R_\mu \Omega_0 \quad (1.5)$$

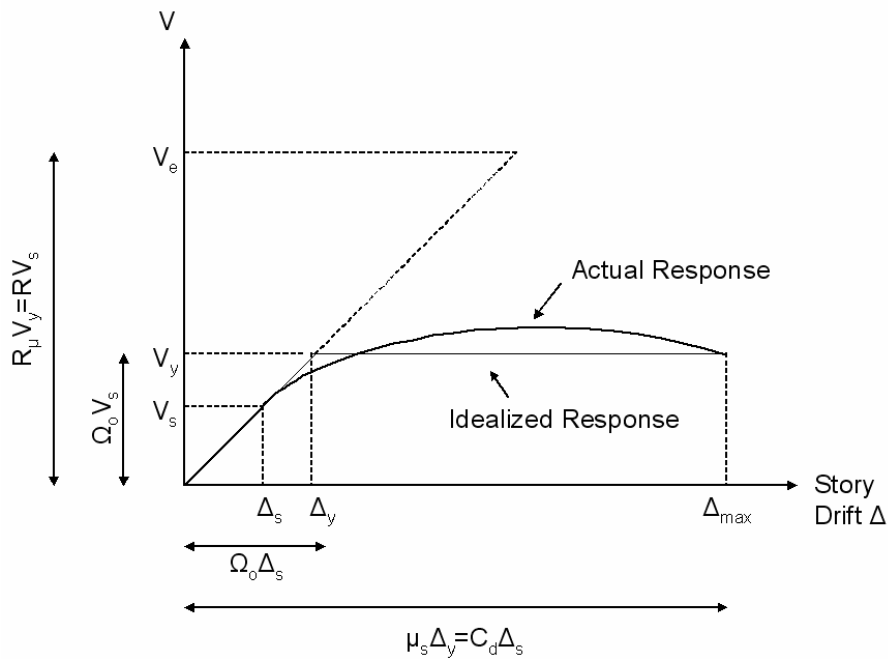


Figure 1.11 - General Structural Response

As mentioned before, the response modification (R), the overstrength (Ω_0), and the displacement amplification (C_d) factors presented in design specifications mostly depend on engineering judgment and on some observations during experiments and past earthquakes. The AISC Seismic Provisions for Structural Steel Buildings [19] recommends a value of 7 for R , 2 for Ω_0 , and 6 for C_d factors for SPSW systems that are not a part of a moment resisting frame system. These values do not depend on the target ductility or the fundamental natural period of the system.

Significant amount of research work has been conducted to quantify ductility reduction factor, R_{μ} . Most of these studies are based on single degree of freedom analysis. A review of pertinent work is presented by Miranda and Bertero [20]. In most of these studies researchers tried to find out relationships between ductility reduction factor (R_{μ}) and structural ductility (μ_s). For almost all of the studies the general consensus is that there is a direct relationship between structural ductility and ductility reduction factor. This relationship is mostly dependent on the natural period of the system, site conditions, and the ground motion characteristics such as maximum ground acceleration, maximum ground velocity, and maximum ground displacement. Researchers [20] argued that design specifications should provide strength reduction factors as a function of structural ductility rather than presenting a single value for a particular system regardless of the target ductility level.

1.2 Objective of the Study

The aim of this study is to explore the dependence of R , Ω_o , C_d for SPSW systems on the ductility level. Pursuant to this goal, a numerical study on these factors using finite element analysis on different cases of SPSW has been conducted. In the following chapters, details of the design procedure and the numerical modeling are given. Results from the numerical analyses are presented for each factor. Finally, the limitations of the study and future research needs are explained.

CHAPTER 2

NUMERICAL STUDY OF SPSW SYSTEMS

2.1 General

A total of 44 SPSW systems were analyzed as a part of this study. The plate thickness, the plate aspect ratio, the number of stories, and the story mass were considered as the prime variables. Plate height was constant for all stories and was taken as 3.0 meters for all wall systems. Plate aspect ratios of 1.0 and 2.0 were considered which cover a wide range of walls between the allowed minimum (0.8) and the maximum (2.5) as per the AISC Seismic Provisions [19]. The infill plate thickness was constant at all stories for the 35 walls. For 9 of the walls, the plate thickness was reduced from the base to the top of the wall.

Plate thickness values of 3.0 mm, 4.5 mm, and 6.0 mm were considered to cover a range of slenderness (plate width divided by thickness) values between 500 and 2000. Two typical floor plans given in Fig. 2.1 were considered. In these floor plans, the SPSW was a part of a framing system that utilized pinned beam to column connections; however, only the horizontal boundary element (HBE) to vertical boundary element (VBE) connections were rigid. Therefore, all of the lateral forces were resisted by the SPSW and the rest of the framing system was primarily utilized for gravity loads.

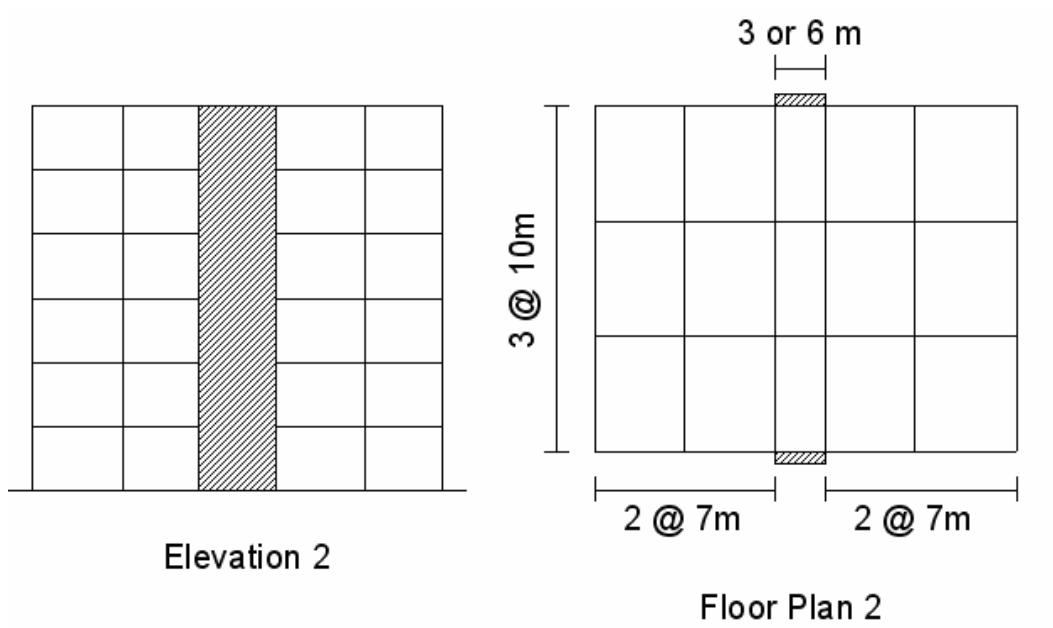
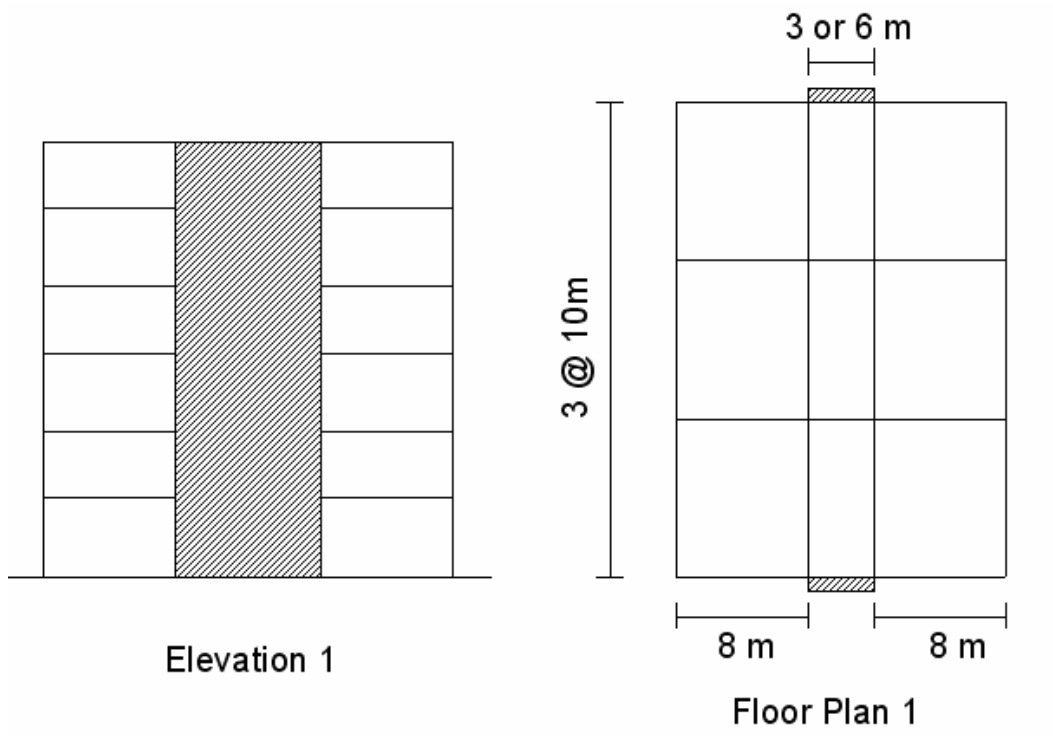


Figure 2.1 - Floor Plans

Dead plus the reduced live load was taken equal to 5kN/m^2 (Metal decking and concrete slab 2.1kN/m^2 ; HVAC 0.5kN/m^2 ; Steel Construction 0.8kN/m^2 ; Partitioning walls 0.5kN/m^2 ; Floor cover 0.5 kN/m^2 ; Reduced live load 0.6 kN/m^2). Based on the tributary areas, mass per story for each wall was calculated as 150 tons and 250 tons for floor plans 1 and 2, respectively. Therefore, for some of the wall geometries, two cases were considered, one with 150 tons of story mass and the other one with 250 tons of story mass. A summary of the walls evaluated in the numerical study and their properties are given in Table 2.1.

Table 2.1 – SPSW Used in the Numerical Study

SPSW #	# of stories	Plate Thickness (mm)	Plate Width (m)	Story Mass (tons)	VBE Section (HD)	VBE Section (W)	Interstory Drift, Δs (%)	Interstory Drift, Δy (%)	α angle (degree)	$\sin 2\alpha$	Fundamental Period (seconds)	V^{design} (kN)
1	2	3	3	150	320 x 158	12x106	0.25	0.53	40	0.99	0.294	1042
2	2	3	6	250	320 x 158	12x106	0.27	0.44	42	1.00	0.265	2105
3	2	6	3	250	400 x 287	14x193	0.24	0.49	39	0.98	0.272	2062
4	2	3,6	3	250	400 x 287	14x193	0.40	0.62	39	0.98	0.299	2062
5	4	3	3	150	400 x 287	14x193	0.24	0.59	41	0.99	0.577	1046
6	4	3	3	250	400 x 287	14x193	0.24	0.59	41	0.99	0.738	1046
7	4	3	6	150	400 x 287	14x193	0.23	0.41	42	0.99	0.384	2102
8	4	3	6	250	400 x 287	14x193	0.23	0.41	42	0.99	0.49	2102
9	4	6	3	150	400 x 551	14x370	0.24	0.52	38	0.98	0.417	2060
10	4	6	3	250	400 x 551	14x370	0.24	0.52	38	0.97	0.531	2060
11	4	6	6	150	400 x 551	14x370	0.23	0.38	39	0.98	0.28	4150
12	4	6	6	250	400 x 551	14x370	0.23	0.38	39	0.98	0.355	4150
13	4	3,6	3	150	400 x 551	14x370	0.34	0.65	38	0.97	0.445	2060
14	4	3,6	6	150	400 x 551	14x370	0.33	0.46	39	0.98	0.304	4150
15	6	3	3	150	400 x 421	14x283	0.26	0.69	41	0.99	0.914	1046
16	6	3	3	250	400 x 421	14x283	0.26	0.69	41	0.99	1.166	1046
17	6	3	6	150	400 x 421	14x283	0.24	0.44	42	0.99	0.588	2099
18	6	3	6	250	400 x 421	14x283	0.24	0.44	42	0.99	0.749	2099
19	6	6	3	150	400 x 744	14x500	0.30	0.69	38	0.97	0.678	2059
20	6	6	3	250	400 x 744	14x500	0.30	0.69	38	0.97	0.858	2059
21	6	6	6	150	400 x 744	14x500	0.26	0.44	39	0.98	0.436	4141
22	6	6	6	250	400 x 744	14x500	0.26	0.44	39	0.98	0.551	4141
23	6	3,4,5,6	3	150	400 x 744	14x500	0.36	0.76	38	0.97	0.708	2059

Table 2.1(continued) – SPSW Used in the Numerical Study

SPSW #	# of stories	Plate Thickness (mm)	Plate Width (m)	Story Mass (tons)	VBE Section (HD)	VBE Section (W)	Interstory Drift, Δs (%)	Interstory Drift, Δy (%)	α angle (degree)	$\sin 2\alpha$	Fundamental Period (seconds)	V^{design} (kN)
24	6	3,4.5,6	6	150	400 x 744	14x500	0.32	0.46	39	0.98	0.463	4141
25	8	3	3	150	400 x 509	14x342	0.29	0.75	41	0.99	1.336	1046
26	8	3	3	250	400 x 509	14x342	0.29	0.75	41	0.99	1.702	1046
27	8	3	6	150	400 x 509	14x342	0.26	0.45	41	0.99	0.833	2098
28	8	3	6	250	400 x 509	14x342	0.26	0.45	41	0.99	1.059	2098
29	8	6	3	150	400 x 990	14x665	0.31	0.73	38	0.97	0.962	2058
30	8	6	3	250	400 x 990	14x665	0.31	0.73	38	0.97	1.212	2058
31	8	6	6	150	400 x 990	14x665	0.27	0.46	39	0.98	0.606	4134
32	8	6	6	250	400 x 990	14x665	0.27	0.46	39	0.98	0.762	4134
33	8	3,4.5,6	3	150	400 x 990	14x665	0.38	0.90	38	0.97	0.989	2058
34	8	3,4.5,6	6	150	400 x 990	14x665	0.31	0.48	39	0.98	0.632	4134
35	10	3	3	150	400 x 634	14x426	0.31	0.91	41	0.99	1.766	1046
36	10	3	3	250	400 x 634	14x426	0.31	0.91	41	0.99	2.244	1046
37	10	3	6	150	400 x 634	14x426	0.26	0.48	41	0.99	1.082	2097
38	10	3	6	250	400 x 634	14x426	0.26	0.48	41	0.99	1.372	2097
39	10	6	3	150	BUILT UP	BUILT UP	0.32	0.73	38	0.97	1.287	2059
40	10	6	3	250	BUILT UP	BUILT UP	0.32	0.73	38	0.97	1.616	2059
41	10	6	6	150	BUILT UP	BUILT UP	0.29	0.50	39	0.98	0.796	4132
42	10	6	6	250	BUILT UP	BUILT UP	0.29	0.50	39	0.98	0.997	4132
43	10	3,4.5,6	3	150	BUILT UP	BUILT UP	0.39	0.90	38	0.97	1.319	2059
44	10	3,4.5,6	6	150	BUILT UP	BUILT UP	0.37	0.56	39	0.98	0.826	4132

2.2 Design of SPSW Systems

Traditionally, the amount of lateral forces has to be known in advance to design the SPSW system. In the present study, the response of SPSW systems subjected to different ground motions was evaluated. Because the same SPSW was subjected to ground motions with different characteristics, the design was conducted in a non-traditional way. Forty-four SPSW systems were designed first without taking into account the amount of lateral forces. Where applicable, the design was conducted in accordance with the AISC Seismic Provisions [19] and AISC Specification for Structural Steel Buildings [21]. According to the AISC Seismic Provisions [19], HBEs and VBEs are designed to remain elastic under maximum forces that can be generated by the fully yielded webs. Only plastic hinging at HBE ends is permitted. With the exception of HBE hinging, in some instances, yielding of the boundary elements is allowed as per the Commentary to AISC [19]. In these cases that are justified by a rational analysis, the yielding of the edge boundary elements will not cause reduction on the SPSW shear capacity to support the demand and will not cause a failure in vertical load carrying capacity.

HBEs and VBEs were designed using European rolled wide flange sections. For all walls, a structural steel grade of S235 [22] (yield stress=235 MPa, ultimate stress=360MPa) was used for the infill plates and S355 [22] (yield stress=355 MPa, ultimate stress=510MPa) was used for the boundary members.

It is well known that the nominal capacity (V_n) of a fully yielded infill plate under shear can be found by:

$$V_n = \frac{1}{\sqrt{3}} F_y t_w L_{cf} \quad (2.1)$$

where; F_y : yield stress, t_w : thickness of infill plate, L_{cf} : clear distance between VBE flanges.

If the plate is too slender then buckling occurs at a stress level much less than the yield stress ($F_y / \sqrt{3}$) under shear. If the plate is restrained, however, as in the case of an SPSW then stresses in excess of buckling stress can be reached due to the formation of a diagonal tension field. The infill plate can be envisioned as a pair of diagonal braces one in tension and the other one in compression. Clearly, the compression diagonal buckles and lateral loads are carried by tension diagonal.

By neglecting the contribution of the compression diagonal and performing a plastic analysis on the panel [16], the shear capacity (V_n) of the web plate after the formation of tension field can be found by:

$$V_n = 0.5F_y L_{cf} t_w \sin 2\alpha \quad , \quad \tan^4 \alpha = \frac{1 + \frac{t_w L}{2A_c}}{1 + t_w h \left(\frac{1}{A_b} + \frac{h^3}{360I_c L} \right)} \quad (2.2)$$

where; α : angle of tension field, h : distance between HBE centerlines, A_b : cross sectional area of HBE, A_c : cross sectional area of VBE, I_c : moment of inertia of VBE taken perpendicular to the direction of the web plate line, L : distance between VBE centerlines.

Equation 2.2 forms the basis of AISC Seismic Provision [19] equations except that the 0.5 coefficient in front is replaced with 0.42. The reason for this change is to incorporate a system overstrength factor of 1.2 into the design expression [16].

HBEs were designed first considering the dead and live loads acting on a tributary area and neglecting the contribution of the infill plate as recommended by the AISC Seismic Provisions [19]. The sections selected were relatively slender. In addition to the gravity loads, HBEs are subjected to flexural forces from boundary frame deformation and to VBE reactions due to the inward force

from the web plate [23]. Because the flexural forces from boundary frame deformation can not be found without knowing the amount of lateral forces, the sizes of HBEs were increased based on engineering judgment. HEA 300 (depth=290mm, flange width=300mm, flange thickness=14mm, and web thickness=8.5mm) was used for all walls and for all stories. In order not to introduce another variable, same size HBE was used for the 3m and the 6m wide walls. However, it should be noted that, this results in an over-design for the 3m wide walls. Commentary to AISC Seismic Provisions [19] recommends that sizeable top and bottom HBE are required to anchor the significant tension fields that develop at the ends of the structural system. In this study, it was assumed that the bottom infill plate was fully anchored to the foundation. Because no specific provisions on sizing the topmost HBE is provided by the AISC Specification [19], the same size HBE (HEA 300) was used for that story.

In designing the VBEs, combined action of gravity loads and loads due to overturning effects were considered. In order to ensure ductile behavior, Commentary to AISC Seismic Provisions [19] recommends that capacity design principles be used in sizing VBEs. There are three methods recommended [19] namely; nonlinear pushover analysis, combined elastic computer programs and capacity design concept, and indirect capacity design approach. These methods require the prior knowledge of the amount of lateral forces produced during an earthquake. In this study, an alternative method for preliminary sizing of VBEs was used. Strictly speaking, this method is non-rigorous and the resulting sizes need to be checked using the sum of the shear strengths of the connected web plates plus the gravity load [23].

In this method, for a particular plate thickness and aspect ratio for the first story infill plate, the nominal shear resistance was calculated using Eqn. 2.2. It should be noted that the sine term was taken equal to unity because the sizes of the VBEs were not known in advance. In fact for most of the wall configurations the angle of inclination of the tension field is above 40 degrees which in turn makes the

sine term greater than 0.98 [14]. Therefore, no error was introduced by this assumption. The nominal shear resistance which corresponds to the base shear resistance was amplified by a factor and distributed as an inverted triangular lateral load over the height of the wall system. An amplification factor of 2.4 was used. The selection of this factor was based on judgment and on some observations from preliminary finite element analyses. The overstrength factor ($\Omega_o=2$) recommended in AISC Specification was increased by 20% to account for the possible increase in base shear capacity due to the following factors. In computing the nominal shear resistance (Eqn. 2.2), the contributions of the boundary frame and the compression diagonal to the lateral load carrying capacity were neglected. Axial loads due to overturning on the VBEs were computed using the amplified lateral loads. The VBE sections were selected using the axial load on the bottom story VBE and the limit state of out-of-plane buckling. The sections selected for each wall system are given in Table 2.1. Due to the large amount of overturning moments, the VBEs were among the heaviest available HD column sections. HD shapes used in Europe are identical to the W shapes used in the United States; hence, in Table 2.1 the US designation is also provided. For some cases no rolled HD shape was suitable; therefore, a built-up section (depth=580mm, flange width=475mm, flange thickness=130mm, and web thickness=90mm) was designed and used in the analyses. For all cases same size VBE was used in all stories resulting in an over-design for the top stories.

After selecting the VBE sizes, a final check was conducted using the procedure explained by Sabelli and Bruneau [23]. In this procedure, the axial load and the moment on the VBE are calculated. The axial load (P_{VBE}) is due to the sum of the shear strengths of the connected web plates plus the gravity load ($P_{gravity}$):

$$P_{VBE} = \sum_{i=1}^{n_s} 0.5F_y t_i h_i \sin 2\alpha + \sum_{i=1}^{n_s} \frac{2M_{p(HBE)}}{L_{cf}} + P_{gravity} \quad (2.3)$$

where, n_s : number of story, $M_{p(HBE)}$: plastic moment capacity of the HBE, h_i : height of the web plate at i^{th} story, t_i : plate thickness at i^{th} story.

The VBE moments (M_{VBE}) are due to the web plate tension and hinging of HBE:

$$M_{VBE} = \frac{F_y t_w h^2 \sin^2 \alpha}{12} + \frac{M_{p(HBE)}}{2} \quad (2.4)$$

After the moment and axial load are found, then the capacity is checked using the beam-column interaction equation presented in AISC Provisions [21]:

$$\frac{P_{VBE}}{P_c} + \frac{8 M_{VBE}}{9 M_c} \leq 1 \quad (2.5)$$

where, P_c and M_c are axial load and moment capacities, respectively as per the AISC Provisions [21].

This procedure was applied to the selected VBE sections and the interaction equation (Eqn. 2.5) ratios were between 0.67 and 1.24 with an average of 0.88. The capacity ratio was well over unity only for SPSW cases 1 and 2 (Table 2.1). Therefore, the sections selected for VBEs are not significantly over-designed or under-designed.

The design base shear (V_{design}) for the SPSW systems was found using Eqn. 2.2 and the values are presented in Table 2.1. It should be noted that the design base shear values do not include the resistance factor (0.9), the system overstrength factor (1.2), and the contribution of the boundary framing to lateral load carrying capacity. In this study, the base shear at first significant yield (V_s) was assumed to be equal to the design base shear (V_{design}).

The fundamental natural periods of the wall systems used in this numerical study were computed using three dimensional finite element analyses. Infill plates, VBEs and HBEs were modeled using 8-node shell elements. Lumped masses were placed at story levels. A commercially available finite element program ANSYS [26] was used to conduct the analysis. An eigenvalue analysis was performed for each case to determine the fundamental natural period of vibration. The details of the numerical procedure to determine the fundamental periods are given in Topkaya and Kurban [24]

According to the values presented in Table 2.1, the fundamental natural period of the wall systems range between 0.265 sec and 2.244 sec.

2.3 Selection of a Suite of Ground Motions

In order to include the variations in ground motion characteristics, 20 earthquake records were selected to be used in the numerical investigation. Earthquake records with differing intensities are expected to produce different levels of ductility demands (such as interstory drift) on a particular wall system. Therefore, earthquake records having peak acceleration values ranging between 0.14g and 1.78g were selected to cover a wide range of peak accelerations. Details of the earthquake records, such as closest distance to fault (CD), peak ground acceleration (PGA) and peak ground velocity values (PGV) are given in Table 2.2. Most of the records were recorded in alluvium sites. This suite of ground motions include both near-field and far-field records. In order to observe inelastic response with various ductility levels, ground motion records should be selected such that the base shear demands are higher than the capacity (V_{design}) of the wall system. The design base acceleration (DBA) for each wall system was obtained by normalizing the design base shear (V_{design}) with the reactive mass. The design base accelerations ($DBAs$), shown with black dots, are plotted against the fundamental natural period of the wall system in Fig. 2.2. In order to produce base shear demands that are higher than the capacity of the wall system (V_{design}), the spectral accelerations of the selected records should be higher than the design base accelerations. On the same figure, the spectral accelerations for 2 percent damping are presented for each ground motion. Examination of this figure reveals that 17 of the records (gm4 to gm20) have spectral acceleration values that are higher than the design base accelerations. On the other hand, three records (gm1 to gm3) were selected such that the spectral accelerations are generally less than the design base accelerations. These three records were used to construct push-over like capacity curves and to quantify the amount of displacements at first yield for a particular wall system.

Table 2.2 – Details of Selected Ground Motion Records

Ground Motion #	Earthquake	Country	Date	Station Location	Site Geology	Mw	CD		PGA		PGV (cm/s)
							(km)	(g)	(g)	(cm/s)	
1	Imperial Valley	USA	15.10.1979	El Centro Array #1, Borcharh Ranch	Alluvium	6.5	22.6	0.14	0.14	16.43	
2	Morgan Hill	USA	24.04.1984	Gilroy Array #2 (Hwy 101 & Bolsa Rd)	Alluvium	6.1	11.8	0.16	0.16	4.99	
3	Northridge	USA	17.01.1994	Downey County Maint. Bldg.	Alluvium	6.7	46.2	0.22	0.22	12.7	
4	Imperial Valley	USA	15.10.1979	Meloland Overpass	Alluvium	6.5	3.1	0.31	0.31	71.77	
5	Northridge	USA	17.01.1994	Saticoy	Alluvium	6.7	12.9	0.37	0.37	28.92	
6	Whittier Narrows	USA	01.10.1987	Cedar Hill Nursery, Tarzana	Alluvium / Siltstone	6.1	41.1	0.41	0.41	19.16	
7	Loma Prieta	USA	18.10.1989	Capitola Fire Station	Alluvium	7	15.9	0.47	0.47	36.15	
8	Northridge	USA	17.01.1994	Rinaldi Receiving Station	Alluvium	6.7	8.6	0.48	0.48	80.33	
9	Northridge	USA	17.01.1994	Katherine Rd, Simi Valley	Alluvium	6.7	14.3	0.51	0.51	44.56	
10	Imperial Valley	USA	15.10.1979	El Centro Array #5, James Road	Alluvium	6.5	5.2	0.55	0.55	49.71	
11	Chi Chi	Taiwan	20.09.1999	CHY028	Soft Soil	7.6	7.31	0.65	0.65	72.78	
12	Cape Mendocino	USA	25.04.1992	Petrolia, General Store	Alluvium	7	15.9	0.66	0.66	89.45	
13	Kobe	Japan	16.01.1995	Takarazu	Soft Soil	6.9	1.2	0.69	0.69	68.28	
14	Kobe	Japan	16.01.1995	Takarazu	Soft Soil	6.9	1.2	0.69	0.69	85.25	
15	Northridge	USA	17.01.1994	Katherine Rd, Simi Valley	Alluvium	6.7	14.3	0.73	0.73	51.11	
16	Düzce	Turkey	12.11.1999	Bolu	Soft Soil	7.1	5.5	0.75	0.75	58.25	
17	Northridge	USA	17.01.1994	Sepulveda VA Hospital	Alluvium	6.7	9.5	0.94	0.94	76.6	
18	Tabas	Iran	16.09.1978	Tabas	Stiff Soil	-	-	1.07	1.07	80.53	
19	Morgan Hill	USA	24.04.1984	Coyote Lake Dam	Rock	6.1	1.5	1.3	1.3	80.79	
20	Northridge	USA	17.01.1994	Tarzana Cedar Hill Nursery	Alluvium	6.7	16.7	1.78	1.78	110.16	

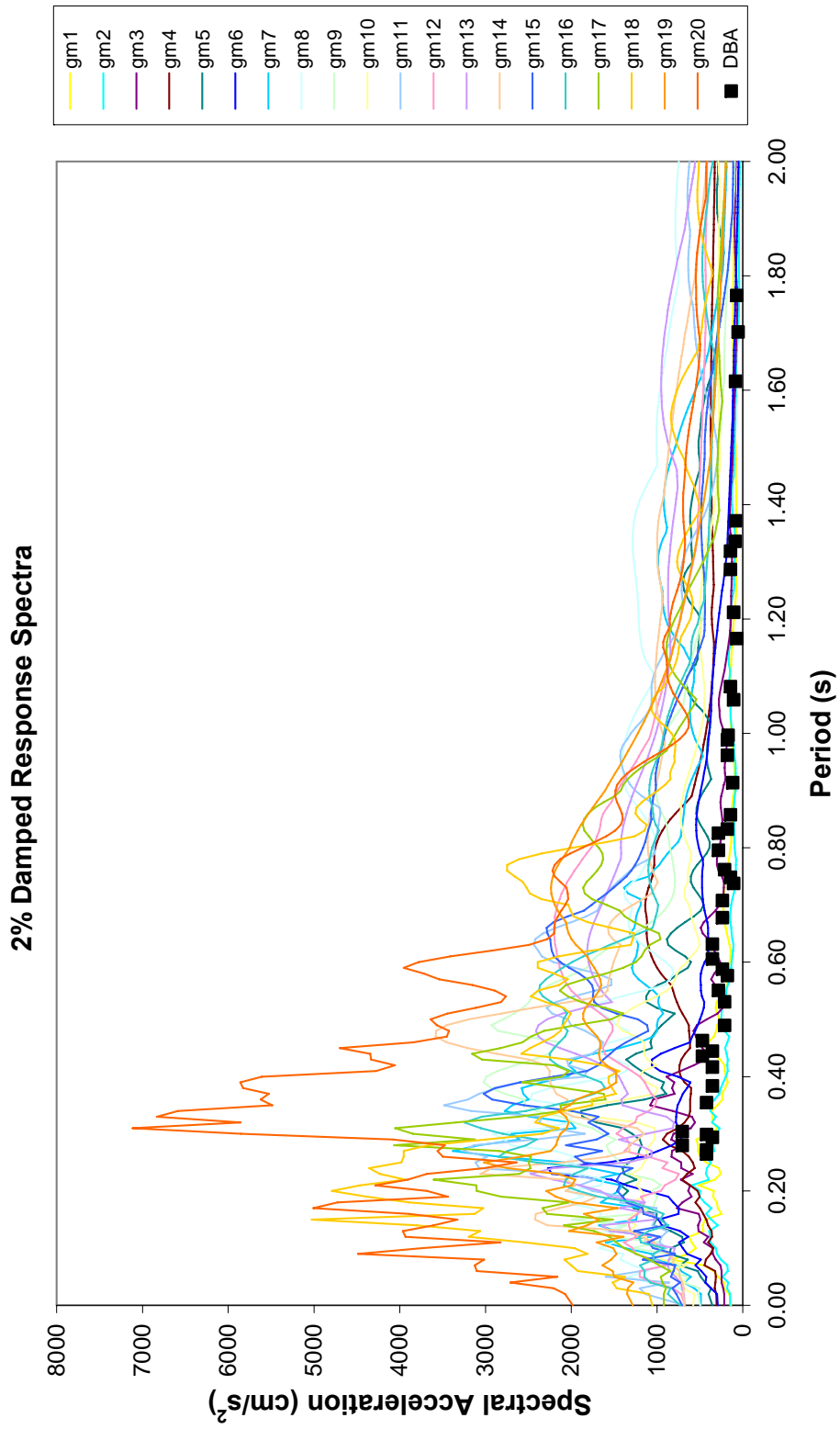
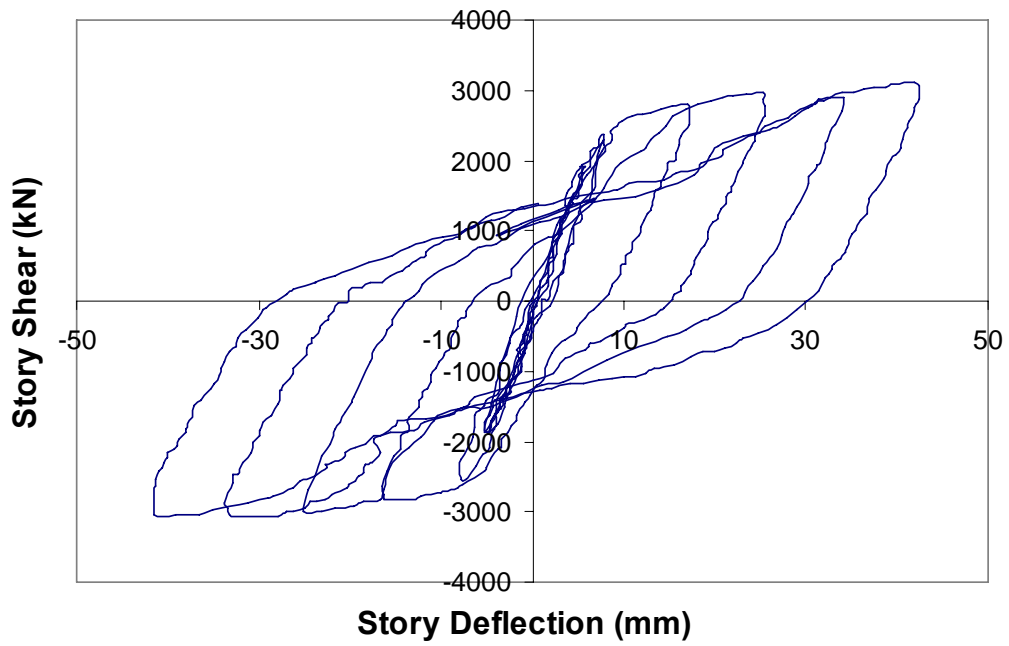


Figure 2.2 – Response Spectra for Selected Earthquake Records and Design Base Acceleration for SPSW

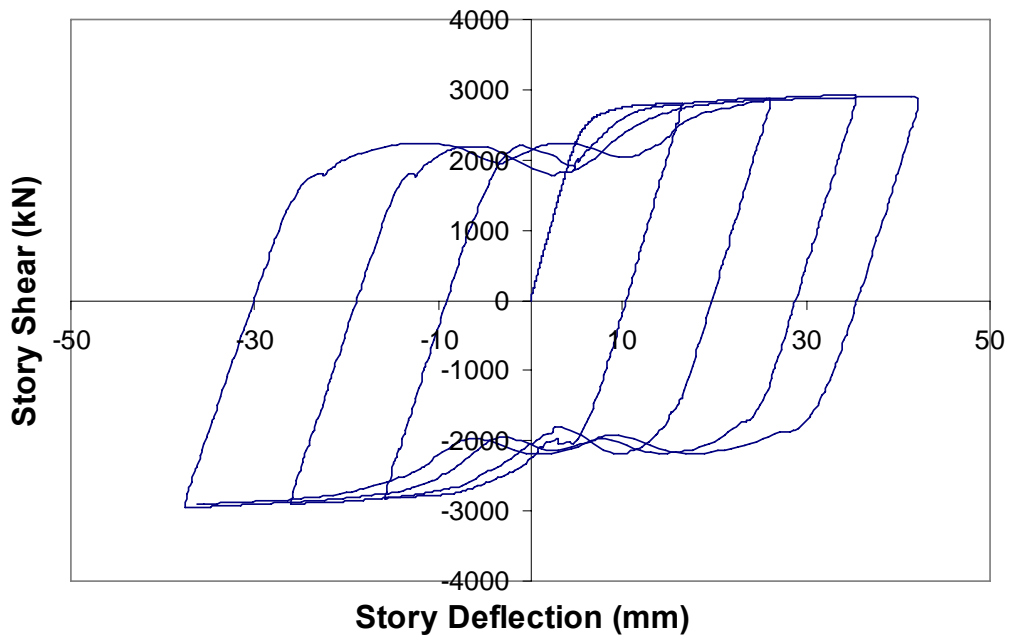
2.4 Finite Element Modeling, Analysis and Verification

The shear force-displacement response of the first story of a four story SPSW tested by Driver et al. [10] is given in Fig. 2.3(a). Examination of this figure reveals that SPSW systems exhibit a complex pinched behavior due to the formation and reorientation of the tension field. In the past, Behbahanifard [25] showed that the behavior of SPSW systems can be simulated using finite element analysis.

In this study, SPSW systems were modeled with three-dimensional finite elements. An explicit finite element code, ANSYS-LSDYNA [26], was used to model and analyze the structures. A typical finite element mesh is given in Fig. 2.4(a). SPSW was modeled using shell elements (shell163). The element type used (shell163) is a 4-node shell element with both bending and membrane capabilities. In all models, webs and flanges of HBEs and VBEs were modeled with one and two shell elements, respectively. Infill plates were modeled with square shell elements having side lengths of 500mm. The mesh density was determined after preliminary analysis. Finer meshes were found to produce numerical instabilities.



(a)



(b)

Figure 2.3 (a) Shear Force – Displacement Response of a SPSW System From the Experiment Performed by Driver et al., 1998 (b) Shear Force – Displacement Response of the Same SPSW System from the Numerical Analysis Performed in This Study

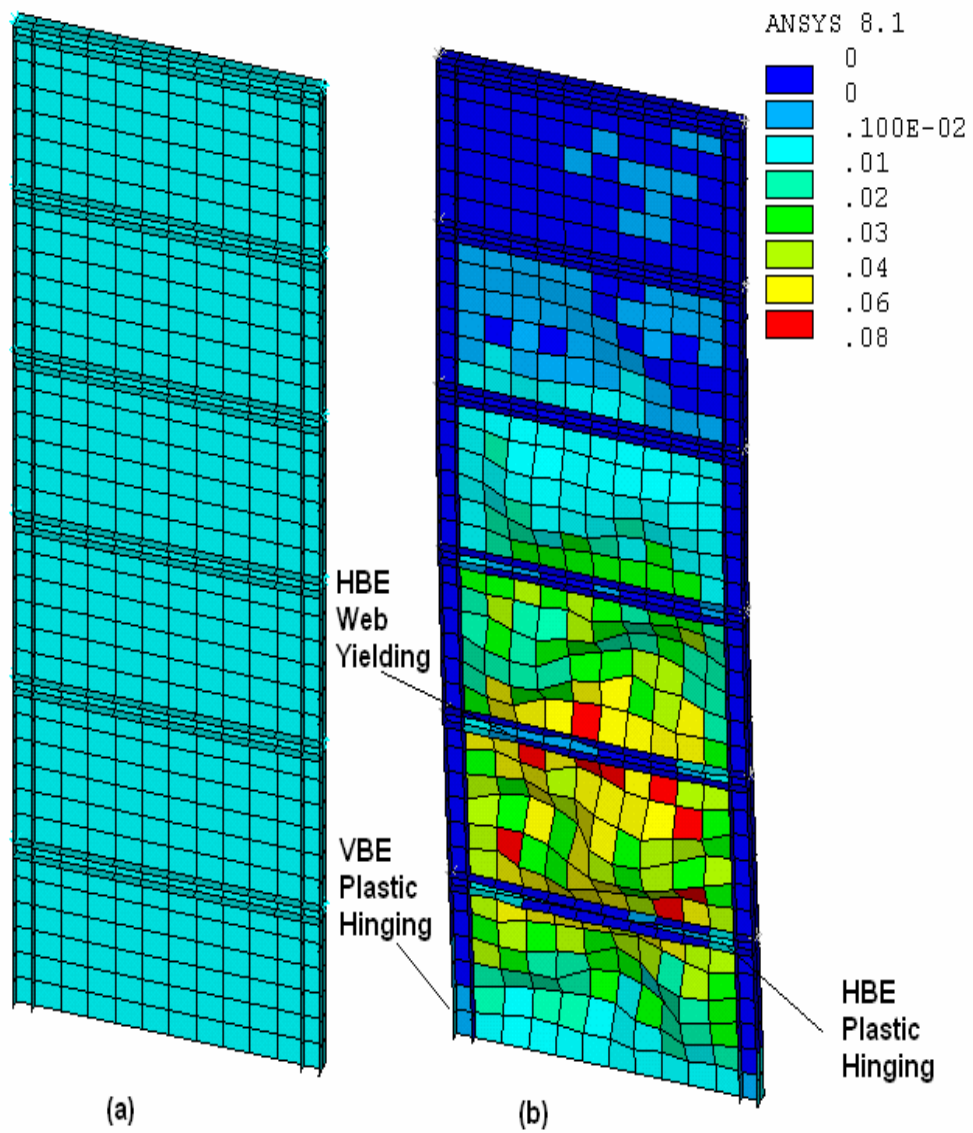


Figure 2.4 (a) A Typical Finite Element Mesh and (b) a Plot of von Mises Equivalent Plastic Strain

Lumped masses were placed at each story level on two nodes. Mass scaling was applied only to the shell elements to speed up the solution. Preliminary analyses revealed that the effect of mass scaling on the results is insignificant. In order to include the post-buckling response of infill plates, geometrical imperfections need to be introduced into the model. This was incorporated by applying a center imperfection of 3mm to the infill plates. Imperfection values that are within fabrication tolerances do not have a major effect on the capacity [25] but are required for analysis purposes.

Displacements of the nodes at the base were restrained against movement and rotation. Out-of-plane movement of the framing was prevented at HBE-VBE intersections for all stories. The nonlinear stress-strain behavior of steel was modeled using von Mises yield criterion with bilinear kinematic hardening. The initial elastic modulus and the hardening modulus were taken as 200 GPa and 1.0 GPa, respectively. Based on cyclic material tests, Shen et al. [27] reported hardening modulus values between 1.0 GPa and 2.8 GPa for a class of structural steels.

The quasi-static analysis of the four story specimen tested by Driver et al. [10] was conducted using the modeling approach presented herein. The shear force displacement response of the first story from numerical analysis is presented in Fig. 2.3(b). Comparisons with the experimental results show that the finite element analysis produces acceptable predictions of the base shear capacity. However, the force-displacement response obtained using numerical analysis is less pinched when compared with the experimental one.

For each set of SPSW system and earthquake record, two time history analyses were conducted. The material nonlinearities were excluded and included for the first and second analysis, respectively. For both analysis cases, geometrical nonlinearities were included to capture the post-buckling response of infill plates.

In all analyses, the axial loads due to gravity were applied to columns first. Then, following the axial loads, ground accelerations were applied to the base of the wall. A two percent mass proportional damping was used in all analysis. Limited amount of shake table tests [28] revealed that stiff SPSW exhibit one percent damping.

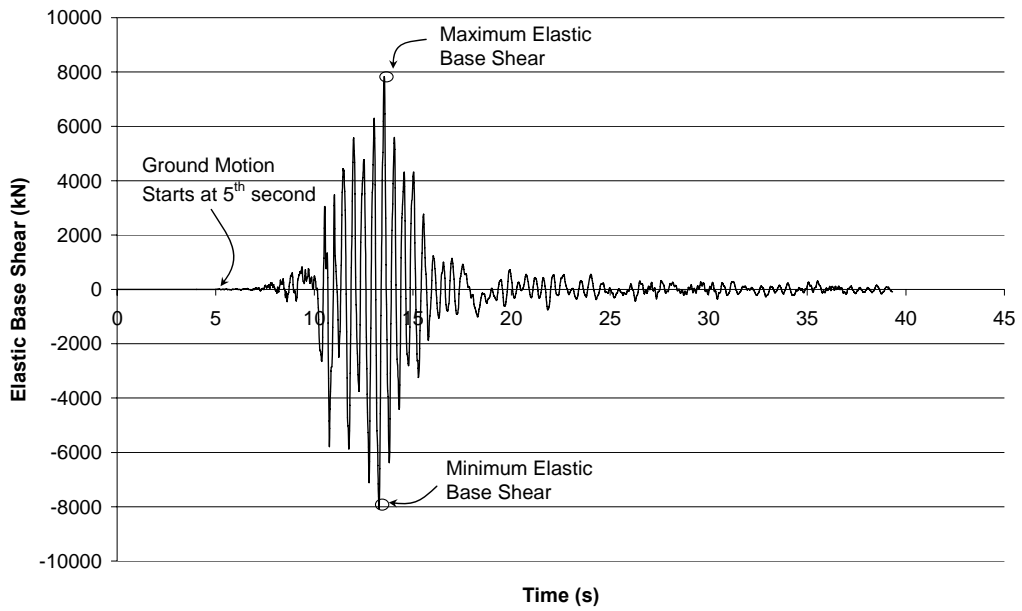
Time step size for analysis ranged between $4.47E-5$ and $7.0E-5$ sec. depending on the smallest element size in the model. During each analysis, the lateral displacements at every story and the base shear were recorded.

CHAPTER 3

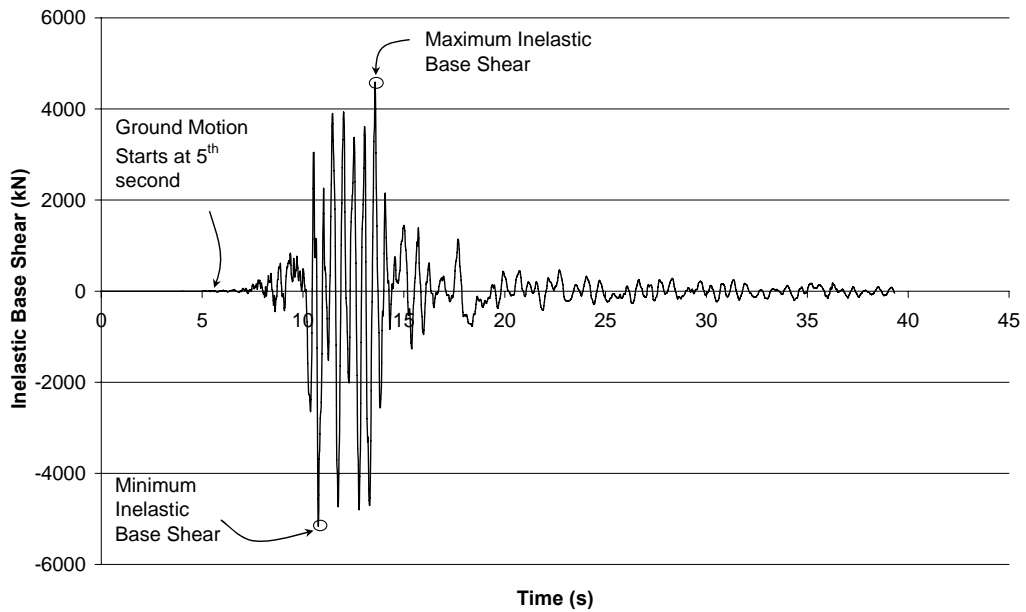
ANALYSIS RESULTS AND FINDINGS

3.1 Results of the Numerical Study

As mentioned before two analyses were conducted for each wall under a ground motion history. A typical elastic and inelastic base shear response is given for a representative 6 story SPSW in Fig. 3.1. For each response history base shear and story displacements are recorded. It is difficult to quantify the ductility level for multi-degree of freedom systems. Usually top story drift [29] is used as an indicator for quantifying ductility levels. Sabelli and Bruneau [23] reported that for SPSW systems with more than three or four stories, the likelihood of yielding all stories simultaneously in the same direction is fairly remote, as higher-mode response becomes more significant. The likelihood is even less, where higher overstrength exists at certain levels [23]. The expected mechanism for taller structures include some concentrations of drift at certain levels [23]. In most of the walls studied herein, high overstrength exists at certain levels due to the constant infill plate thickness and the same size VBE used for all stories. When a typical response of a SPSW from numerical analysis was examined, it was observed that yielding was localized at particular stories as reported by Sabelli and Bruneau [23]. For example, in the case of a six story SPSW shown in Fig. 2.4(b), yielding is localized at first four stories and the maximum amount of interstory drift is 1.7%, 2.3%, 1.7%, 0.8%, 0.3%, 0.4% for 1st, 2nd, 3rd, 4th, 5th, 6th, stories, respectively. Based on these observations, it was decided to use the maximum interstory drift ratio (*MISDR*) as an index to quantify ductility demands of SPSW systems investigated in this study. In fact, in most of the experimental studies, interstory drift ratio was used to establish damage levels for SPSW systems.



(a)



(b)

Figure 3.1 (a) A Typical Elastic(a) and Inelastic(b) Base Shear Response for a Representative 6 Story SPSW

For each wall geometry, pushover-like curves were constructed by utilizing the 20 ground motion records as shown in Fig. 3.2. According to the procedure given by Uang [18], an elastic perfectly plastic curve was fitted to the data and interstory drift ratios at design level (i.e. first significant yield) (Δ_s) and at structural yield level (Δ_y) were determined using this curve. Interstory drift ratios Δ_s and Δ_y for each wall are given in Table 2.1 in terms of percentages. For the 44 walls, Δ_s values range between 0.23% and 0.40%, having a mean value of 0.29%. On the other hand, Δ_y values range between 0.38% and 0.91%, having a mean value of 0.59%.

In order to observe yielding patterns, for each wall, the analysis under the ground motion record which produces the highest amount of interstory drift was considered. In general, for the 44 walls considered either of the ground motions 11, 12, 19, or 20 (Table 2.2) produced the highest interstory drift demands. For each wall, the von Mises equivalent plastic strain distribution (Fig. 2.4(b)) was plotted after the analysis. Observations of the strain plots revealed that for SPSW 1 and 2, a soft story mechanism was developed by hinging at top and bottom of VBE. For all other walls, yielding of infill plates and hinging of HBE ends at particular stories were observed (Fig. 2.4(b)). In general, for most of the walls, VBE hinging at the base or partial yielding of the outermost VBE flanges were present. In most of the cases, web yielding (Fig. 2.4(b)) of HBE was also observed. Although web yielding and VBE hinging at the base are not desirable as per the AISC Specification [19], these do not adversely affect the lateral and gravity load carrying capacity. In neither of the analysis, global buckling of VBES was detected. Failure of the topmost HBE due to the tension field forces was observed for 5 plate walls (3,4,13,23,33). These walls, in general, have a plate width of 3 m and have variable infill plate thickness.

Four Story SPSW With 3mm Plate Thickness, 3m Plate Width and 150 tons of mass per story

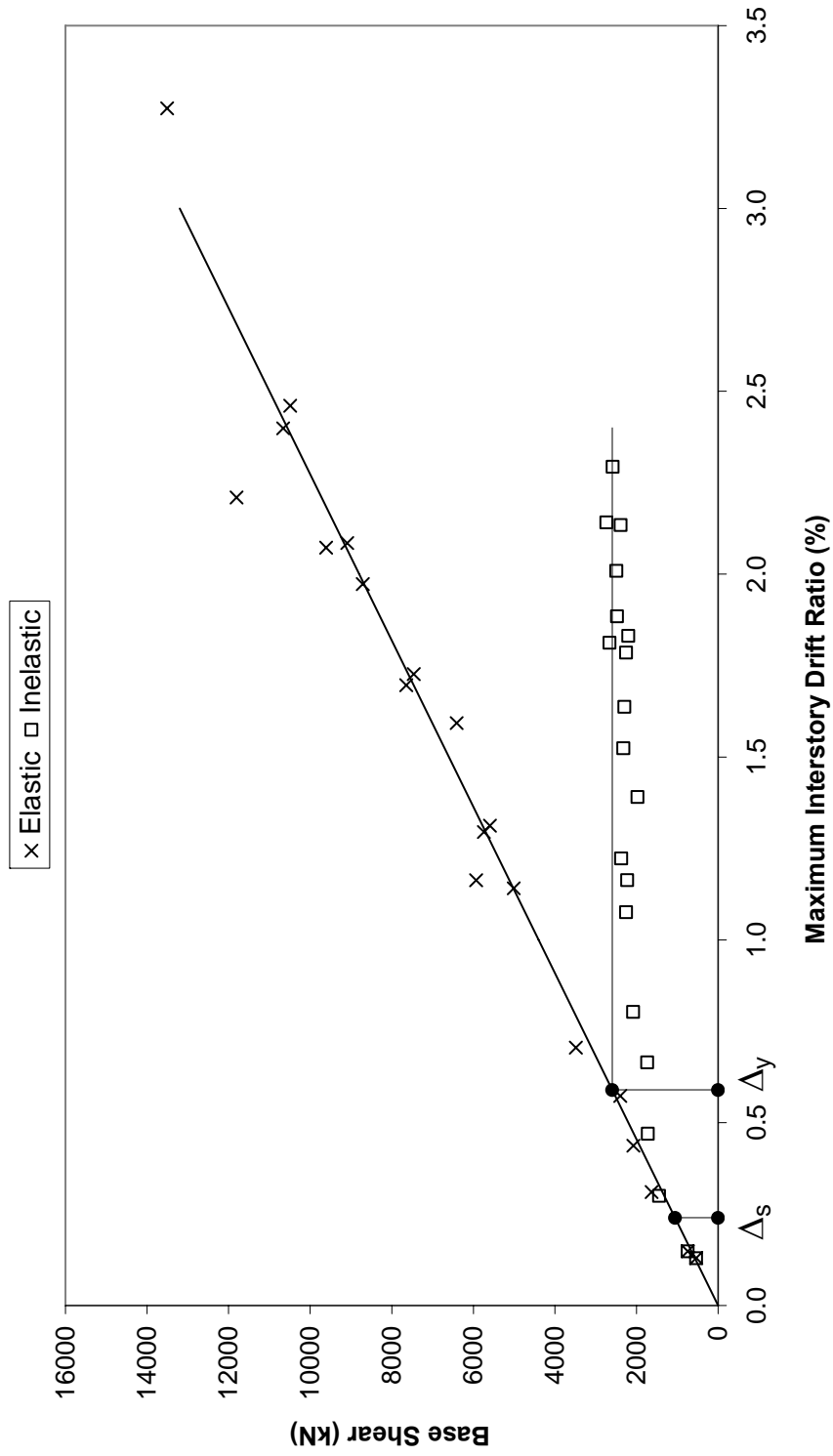


Figure 3.2 – Pushover Like Curve

Following sections present details of findings for each factor. Wherever possible, mean value, upper and lower bound expressions based on maximum interstory drift ratio (*MISDR*) were developed to quantify the behavior. Coefficients were rounded off for simplicity.

3.1.1 Overstrength Factor (Ω_o)

Several factors contribute to the overstrength of a structural system such as the internal force redistribution (redundancy), higher material strength than those specified in design, strain hardening, member oversize, deflection constraints, multiple loading combinations, effect of nonstructural elements, and etc. The overstrength factor based on nominal material properties can be denoted by Ω_n . The relationship between the structural overstrength (Ω_o) and the overstrength (Ω_n) based on nominal material properties is represented as follows [18]:

$$\Omega_o = \Omega_n F_1 F_2 \dots F_n \quad (3.1)$$

where, F_1, F_2, \dots, F_n : factors used to account for the actual material properties such as the difference between actual static yield strength and nominal yield strength, strain rate effect during an earthquake excitation, and etc.

The overstrength of a SPSW can be determined either by inelastic static analysis or by nonlinear time history analysis. The aim of the inelastic static analysis procedures is to estimate the base shear at structural collapse level (V_y) and at first significant yield (V_s). Computer based pushover analysis or a number of hand methods such as Plate Frame Interaction (PFI) [14], Modified Plate Frame Interaction (MPFI) [30], and virtual work method [16] can be used to find these base shear values. The drawback of these methods is that the base shear at collapse level (V_y) is dependent on the assumed lateral load profile. On the other hand, pushover like curves (Fig. 3.2) based on nonlinear time history analysis can be used to estimate the structural overstrength. In this case, however, the value of V_y is dependent on the ground motion characteristics.

Sabouri-Ghomi and Roberts [1-4] have shown that after the web plate yields, the lateral loads are carried by the frame action of the VBE and HBE. Therefore, the overstrength of a SPSW system is significantly influenced by the capacity of its boundary elements. Berman and Bruneau [16] have identified two important collapse mechanisms, namely, the soft story mechanism and the uniform yielding mechanism. The base shear at the structural collapse level (V_y) can be calculated by summing the strength of the web plate and that of the boundary elements [16]. In soft story mechanism, the plastic hinges that would form in the vertical boundary elements can be included in the capacity expression. The shear at a particular story that would cause a soft story mechanism can be found as follows [16]:

$$V_y = 0.5F_y t_i L_{cf} \sin 2\alpha + \frac{4M_{p(VBE)}}{h_{si}} \quad (3.2)$$

where, $M_{p(VBE)}$: plastic moment capacity of the VBE at the soft story, h_{si} : height of the soft story.

Similarly, plastic hinges at the HBE ends and at the base of the VBE form in the uniform yielding mechanism. The base shear strength based on this failure mode can be calculated as follows [16]:

$$V_y = \frac{\sum_{i=1}^{n_s} 0.5F_y L_{cf} h_{bi} (t_i - t_{i+1}) \sin 2\alpha + n_s 2M_{p(HBE)} + 2M_{p(VBE)}}{ch_T} \quad (3.3)$$

where, h_{bi} : height of the i^{th} story from the base, h_T : total height of the wall, c : a coefficient depending on the distribution of lateral loads (0.5 for equal lateral, and 0.67 for triangular distribution). It should be noted that Eqn. 3.3 is valid for walls having the same size HBE at all stories and the plastic moment capacity of HBE at the top floor is less than the plastic moment capacity of the VBE. Berman and Bruneau [16] reported that the actual failure mechanism is typically somewhere between a soft-story mechanism and uniform yielding of the plates on all stories.

The expected base shear at collapse level (V_y) was calculated for the 44 plate walls using Eqns. 3.2 and 3.3. A triangular lateral load distribution ($c=0.67$) was assumed during the calculations. It was observed that for all walls, except 1 and 2, the uniform yielding mechanism gives lower base shear values when compared with the soft story mechanism. The base shear at the collapse level (V_y) obtained from Eqns. 3.2 and 3.3 was normalized by the base shear at first significant yield found by making use of Eqn. 2.2. The normalized value represents the expected structural overstrength with nominal material properties (Ω_n). When the values were examined, it was observed that the 3m wide walls have higher overstrength compared to 6m wide walls. The average overstrength values are 2.16 and 1.79 for the 3m and the 6m wide walls, respectively. The standard deviations in overstrength values are 0.20 and 0.17 for the 3m and the 6m walls, respectively. For a particular material strength and plate thickness, walls with 3m and 6m plate width essentially have the same size VBE. Although a 6m wide plate has twice the capacity of a 3m wide plate, the overturning moment effects on the VBE are the same for both cases due to the increased moment arm associated with the 6m wide plate. As mentioned before, the same size HBE (HEA 300) was used for all walls. For a particular plate thickness, the framing (combined HBE and VBE) is the same for both the 6m and the 3m wide walls. When same size framing is used, obviously the capacity increase is much more pronounced for the 3m wide plate case as opposed to the 6m wide plate case.

In order to evaluate the overstrength values obtained from nonlinear time history analysis, the interstory drifts Δ_s and Δ_y given in Table 2.1 were considered. The ratio of Δ_y to Δ_s is equivalent to the ratio of V_y to V_s which is the overstrength according to Eqn. 1.3. The average overstrength values from nonlinear time history analysis are 2.29 and 1.65 for the 3m and 6m wide walls, respectively. When all walls are considered, an average overstrength value of 2.1 is obtained. Average overstrength values from nonlinear time history analysis and inelastic static analysis are close to each other. The differences can be attributable to the

differences in lateral load profiles. In deriving Eqn. 3.3, which is based on virtual work principles, only a single mode of vibration is considered. Higher mode effects are not accounted for in Eqn. 3.3 but are included in the nonlinear time history analyses.

It is worthwhile to reiterate that the values presented so far are for structural overstrength with nominal material properties (Ω_n). If the plate or the boundary member materials possess higher yield strength, then this can further increase the overstrength of the system. Eqn. 3.1 can be used to estimate the overstrength (Ω_o) value that includes the overstrength in materials. Structural overstrength (Ω_n) can be amplified by the material overstrength factor (Ratio of expected yield stress to the specified minimum yield stress) presented in design specifications. Representative values given in the AISC Seismic Provisions [19] are 1.5, 1.3, and 1.1 for ASTM A36, ASTM A572 Gr42, and ASTM A572 Gr50 steels, respectively.

3.1.2 Ductility Reduction Factor (R_μ)

In most of the earlier studies [20] on single degree of freedom systems, researchers established the relationship of $R_\mu = \mu_s$ for long period structures (usually $T > 0.5$ sec). For short period structures, there is a general consensus that R_μ is less than μ_s .

The dependence of R_μ on μ_s was examined based on the numerical analysis results. When the ductility reduction factor is plotted against structural ductility as in Fig. 3.3 a large scatter in results is observed. It should be mentioned that despite this scatter the best line fit to the data has a slope of 0.94 showing $R_\mu = \mu_s$ trend. In the present study, there are a few walls that have a fundamental period less than 0.5 sec. Due to the insufficient number of data points and the scatter in

results, no conclusions can be derived for the dependence of R_μ on μ_s for $T < 0.5$ sec.

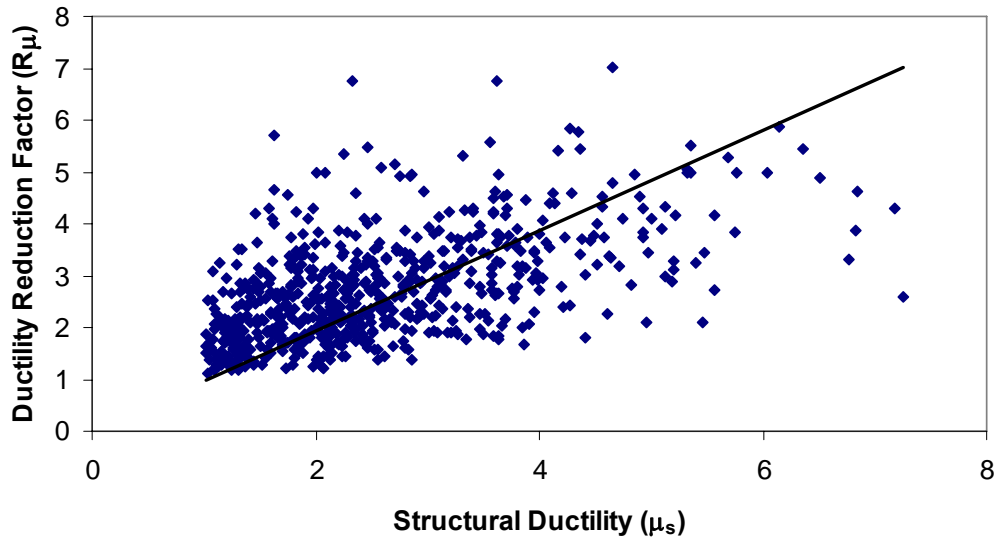


Figure 3.3 - Ductility Reduction Factor Against Structural Ductility

A plot of ductility reduction factor (R_μ) as a function of maximum interstory drift ratio ($MISDR$) is given in Fig. 3.4. It is evident from this figure that there is large scatter due to the variability in structural and ground motion characteristics. Based on 680 data points with $MISDR > 0.5\%$, the following set of equations can be used to quantify the analysis results:

$$\begin{aligned}
 R_\mu &= 1.7ISDR \quad (\text{Mean}) \\
 R_\mu &= 2.5ISDR \quad (\text{Upper Bound}) \\
 R_\mu &= 1.0ISDR \quad (\text{Lower Bound})
 \end{aligned} \tag{3.4}$$

Mean value, lower and upper bounds are given in Fig. 3.4. This set of equations ensure that 80 percent of the data points are within the bounds.

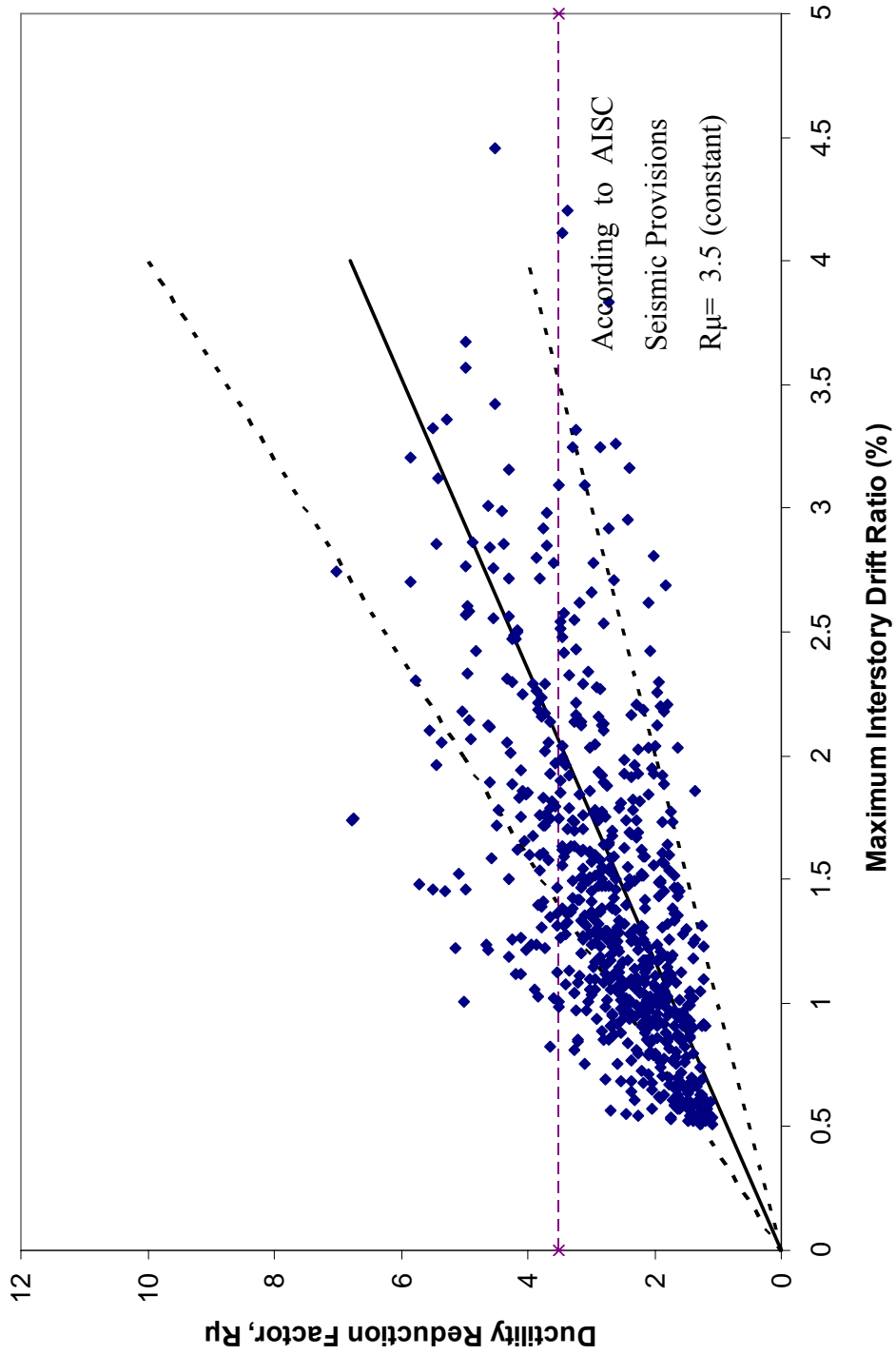


Figure 3.4 – Variation of Ductility Reduction Factor With MISDR

3.1.3 Response Modification Factor (R)

Response modification factor is a combination of the overstrength factor and the ductility reduction factor. Conclusions related to ductility reduction factor can be used for the response modification factor. In Fig. 3.5, response modification factor is plotted against the maximum interstory drift ratio. Although there is large scatter in data, it is observed that R value increases with the interstory drift ratio. Based on 880 data points, the following set of equations can be used to quantify the analysis results:

$$\begin{aligned} R &= 3.57ISDR \text{ (Mean),} \\ R &= 5.25ISDR \text{ (Upper Bound)} \\ R &= 2.10ISDR \text{ (Lower Bound)} \end{aligned} \tag{3.5}$$

Mean value, lower and upper bounds are given in Fig. 3.5. This set of equations ensure that 85 percent of the data points are within the bounds. The coefficient of determination (R^2) for the best line is 0.67. It should be noted that the response modification factor (R) values presented in Fig. 3.5 were obtained using analyses with nominal material properties.

The response modification factor (R) recommended by AISC Seismic Provisions [19], which is equal to 7.0, is also shown in the figure. When that value is used the expected maximum interstory drift ratio will be 1.96 %.

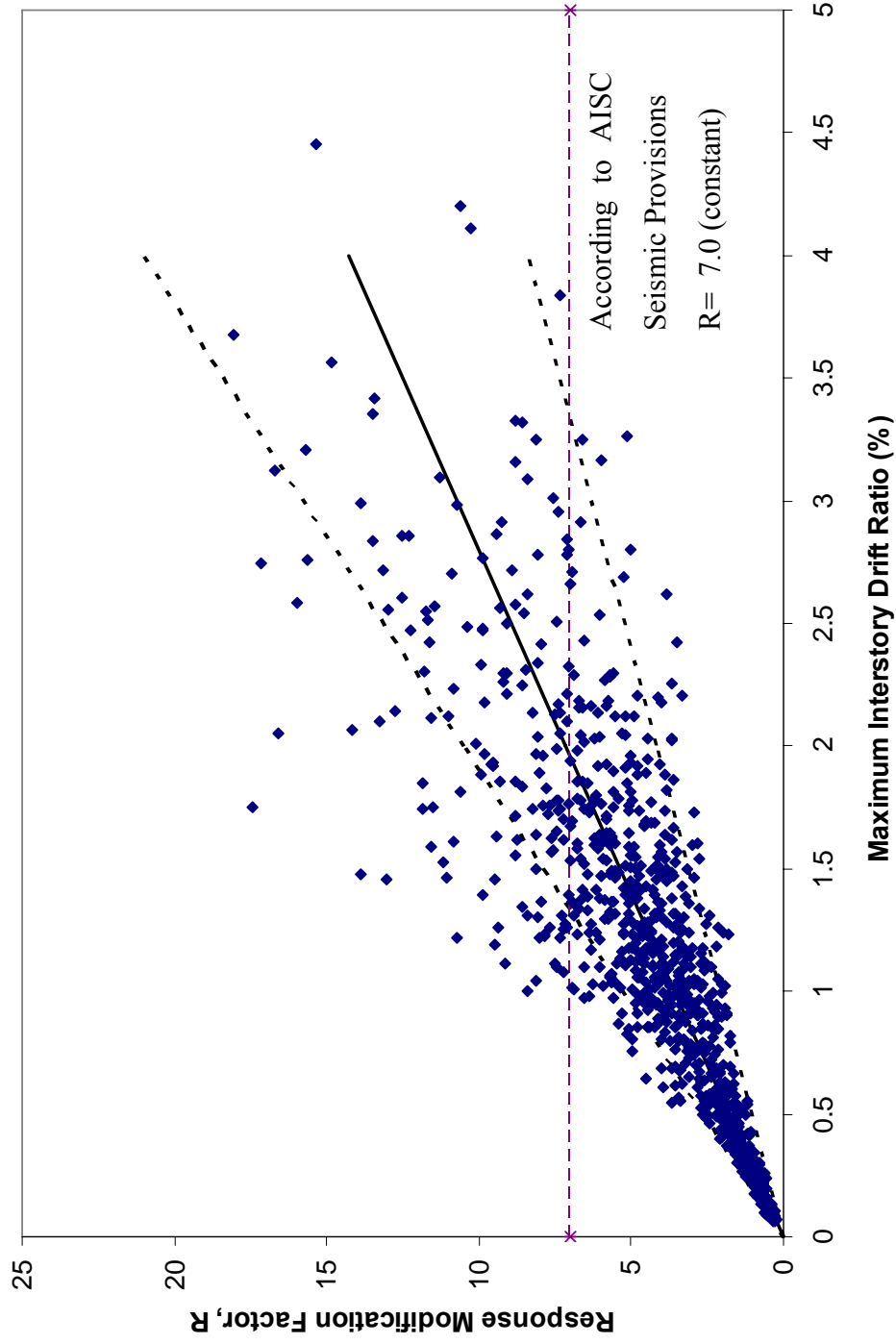


Figure 3.5 – Variation of Response Modification Factor With MISDR

3.1.4 Displacement Amplification Factor (C_d)

Displacement amplification factor (C_d) is used to find the amount of inelastic displacements that a structure experiences using elastic displacements. By making use of this factor, designers can predict the maximum amount of inelastic displacement by conducting an elastic analysis only. Observations from single degree of freedom analysis reveal that equal displacement rule is present for long period structures. This means that the amount of displacement if the structure remains elastic is equivalent to the amount of displacement considering yielding. The applicability of this finding to the SPSW systems considered herein was investigated. As mentioned before, for the SPSW systems studied, yielding was localized at particular stories. Therefore, the ratio of the maximum inelastic interstory drift to the maximum elastic interstory drift was considered. It should be noted that the maximum interstory drift does not necessarily occur at the same story for the inelastic and elastic analysis. The relationship between the ratio of inelastic to elastic displacements and the fundamental natural period of the system was explored. The ratio of the maximum interstory drift obtained by conducting inelastic and elastic analysis is plotted against the fundamental natural period of the system in Fig. 3.6. Examination of this figure reveals that the equal displacement rule holds for systems having a fundamental natural period greater than 0.5 sec. The displacement ratios fall within a band of 0.5 and 1.5, having a mean close to unity, in the long period range ($T > 0.5$ sec). For structures having a fundamental natural period less than 0.5 sec, inelastic displacements can reach to 2.5 times the elastic displacements. Moreover, C_1 factors (modification factor to relate expected maximum inelastic displacements calculated for linear elastic response) in FEMA 356 [33] for site class B and for different T_s values (characteristic period of the response spectrum) were calculated for different fundamental periods and shown in Fig 3.6. As it is seen, the trend of the data points resembles the trend of C_1 values and the mean of the data points are close to C_1 values calculated using 0.5 second as T_s value.

The amount of displacement amplification is related to the amount of ductility that the structure experiences. In order to quantify the C_d value, displacement amplification (the inelastic interstory drift normalized by the interstory drift at first significant yield) values are plotted against the response modification factor (R) values in Fig. 3.7. Although there is large scatter in data, the increase in C_d with R is observed. Based on 880 data points, the following set of equations can be used to quantify the analysis results:

$$\begin{aligned}
 C_d &= 0.9R \quad (\text{Mean}) \\
 C_d &= 1.5R \quad (\text{Upper Bound}) \\
 C_d &= 0.5R \quad (\text{Lower Bound})
 \end{aligned}
 \tag{3.6}$$

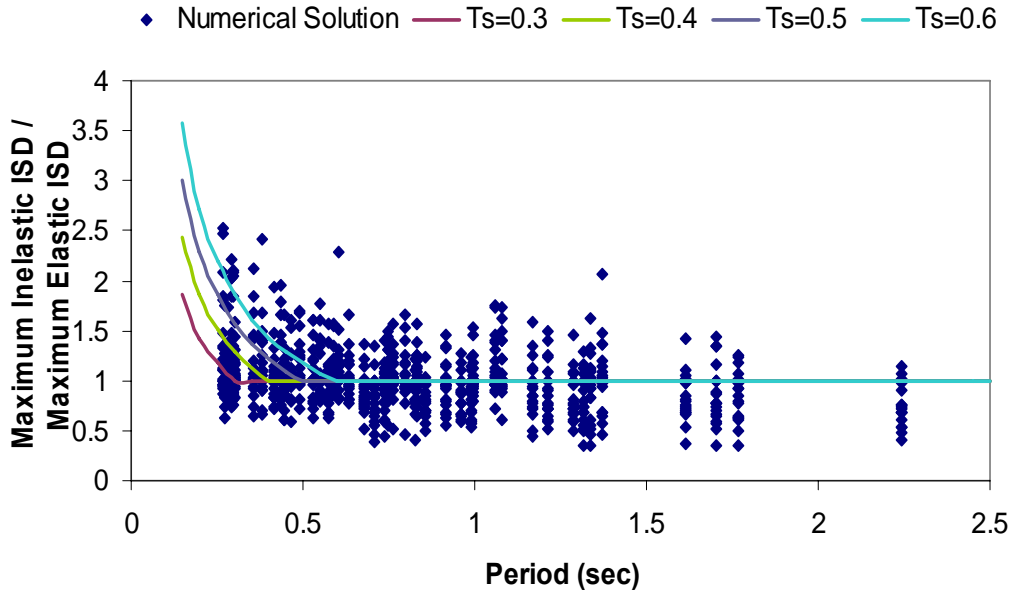


Figure 3.6 - The Ratio of the Maximum Interstory Drift Obtained By Conducting Inelastic and Elastic Analysis Against the Fundamental Natural Period of the System

Mean value, lower and upper bounds are given in Fig. 3.7. This set of equations ensure that 90 percent of the data points are within the bounds. The coefficient of determination (R^2) for the best line is 0.63. Additionally, the displacement amplification factor (C_d) recommended by AISC Seismic Provisions [19], which is equal to 6.0, is also shown in the figure. When the response modification factor (R) value recommended by recommended by AISC Seismic Provisions [19] is used, the expected C_d value will be 6.3 according to equation 3.6. The value is close to the one recommended by AISC [19].

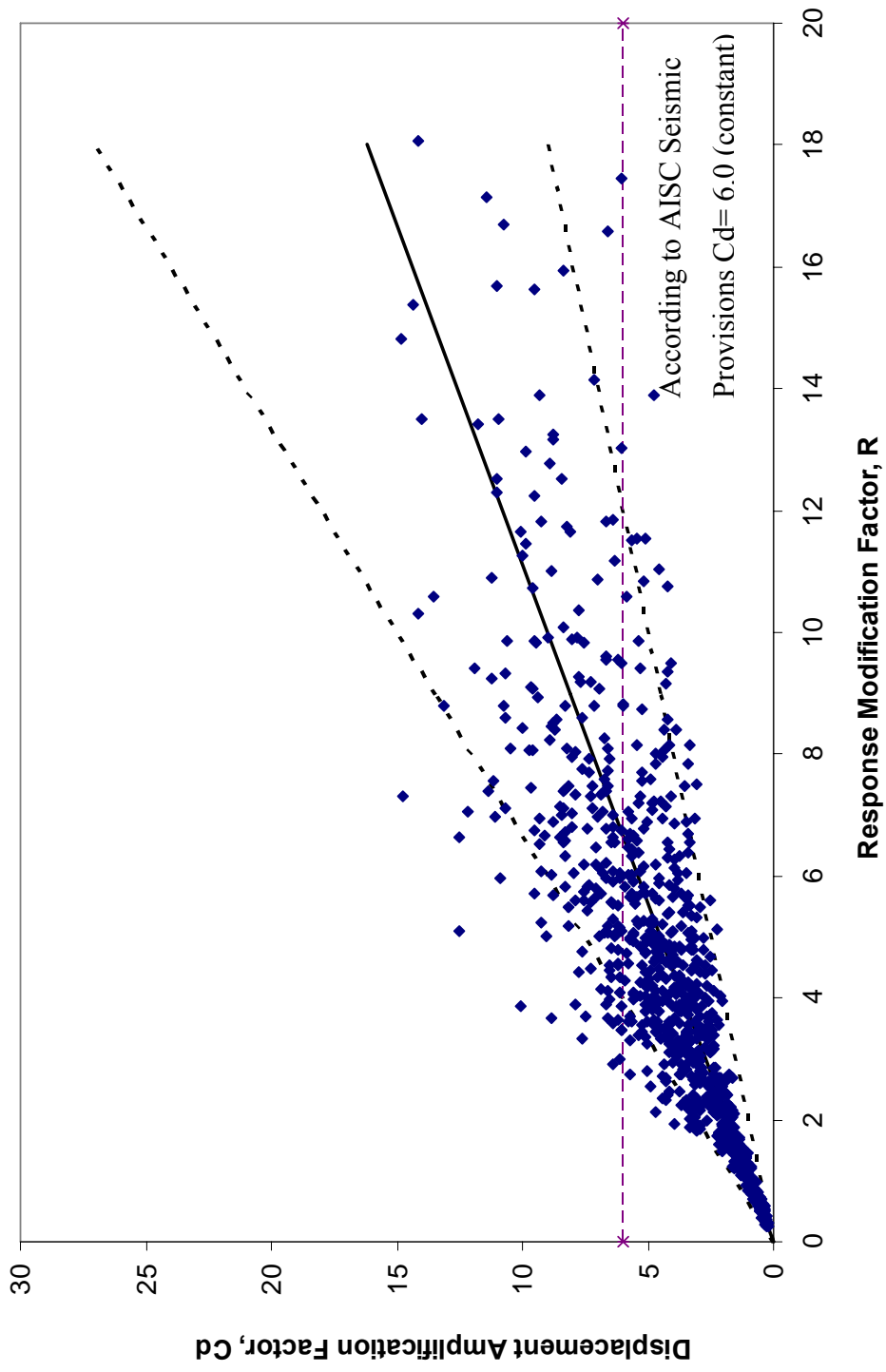


Figure 3.7 – Variation of Displacement Amplification Factor With Response Modification Factor

CHAPTER 4

LIMITATIONS, SUMMARY AND CONCLUSIONS OF THE STUDY

4.1 Limitations of the Study and Future Research Needs

The author recognizes that the results presented in this thesis cannot be generalized. The factors studied, are more and less affected by different parameters such as: the residual stresses, the redundancy, the material hardening, the welding property, the weld flaw, the formation of cracks, and many other parameters that are related and dependent to the construction practice, design methodology, and material properties. These parameters are not easily modeled using commonly employed finite element models. Investigating such factors using the finite element modeling without considering or modeling these parameters will result in an outcome that is limited and less representing the actual structural behavior of the system.

The design methodology adopted in Chapter 2 is not the conventional design approach. In particular, same size VBE was used for all stories, formation of partial tension field action was allowed at the top story, and same size HBE was used at all stories and for different plate widths. Bilinear kinematic hardening was assumed in the analysis and formation of cracks on infill plates was not modeled. All analysis results, in particular the ductility values, were based on nominal material properties and does not represent the actual properties of steel.

Future research should consider SPSW systems that are a part of moment resisting systems. In addition, design methodologies other than the one used in this study require further investigation.

4.2. Summary and Conclusions

Response modification (R), ductility reduction (R_μ), overstrength (Ω_o), and displacement amplification (C_d) factors for 44 SPSW systems were investigated through numerical analyses. A parametric study that employs three dimensional nonlinear finite element time history analyses has been undertaken. In the parametric study variation in wall geometry, natural period of vibration and ground motion characteristics were taken into account. SPSW systems used in this study were all designed based on capacity design principles and they are not part of a moment resisting frame system. Based on the analysis results dependence of aforementioned factors on performance parameters was evaluated. Maximum interstory drift was selected as the performance criterion because most of the inelastic deformations are controlled at a particular story due to significant amount of yielding in the infill plates. Dependence of ductility reduction and response modification on maximum interstory drift ratio ($MISDR$) was established. Analysis results revealed that these factors are correlated; however, there is wide scatter in the values due to the variations in ground motion characteristics.

The overstrength present for the walls can be estimated by considering the uniform yielding mechanism and the soft story mechanism. Due to the presence of higher mode effects, overstrength values from numerical analysis are slightly different than the ones obtained using mechanism solutions. The response modification (R), and the ductility reduction (R_μ) were related to the maximum interstory drift ratio ($MISDR$). Mean value, upper and lower bound equations were developed to quantify the analysis results. The use of these equations are two fold; to estimate the amount of maximum interstory drift ratio expected for a SPSW system designed using a particular value of R , and to find out the range of R values that can be used for a target interstory drift level. Finally, the relationship between C_d and R was established and analysis results are quantified using mean value, upper and lower bound equations.

The following can be concluded from this study:

- There is significant amount of overstrength present for SPSW systems because of the frame action since HBEs and VBEs are designed to remain elastic under maximum forces that can be generated by the fully yielded webs and HBEs are rigidly connected to VBEs. An overstrength factor (Ω_n) with nominal material properties 2.1 is recommended for these systems. The overall overstrength factor (Ω_o) if material overstrength is considered varies between 2.3 and 3.2. (Using material overstrength factors recommended by AISC Seismic Provisions [19])
- Structural ductility (μ_s) of SPSW systems are quantified by normalizing the maximum interstory drift with the interstory drift at structural yield. It is found that the ductility reduction (R_μ) factor is equivalent to structural ductility (μ_s) for long period structures ($T > 0.5$ sec). Expressions (Eqn. 3.4) are developed to relate ductility reduction factor to maximum interstory drift.
- Expressions (Eqn. 3.5) are developed to relate response modification factor to maximum interstory drift. Mean value, upper and lower bound expressions presented in Eqn. 3.5 can be used to estimate the amount of maximum interstory drift demand given a particular value of R . These expressions are based on nominal material strength and need to be magnified by material factors if yield strength of the material is higher than the ones assumed in design.
- Dependence of the displacement amplification factor on the response modification factor is established. Expressions (Eqn. 3.6) are developed to predict displacement amplification for a given R value.

REFERENCES

- [1] Sabouri-Ghomi S, Roberts TM. Nonlinear dynamic analysis of thin steel plate shear walls. *Computers and Structures*, 1991; 39(1/2): 121-127.
- [2] Roberts TM, Sabouri-Ghomi S. Hysteretic characteristics of unstiffened perforated steel plate shear panels. *Thin-Walled Structures*, 1992; 14(2): 139-151.
- [3] Sabouri-Ghomi S, Roberts TM. Nonlinear dynamic analysis of steel plate shear walls including shear and bending deformations. *Engineering Structures*, 1992; 14(5): 309-317.
- [4] Roberts TM. Seismic resistance of steel plate shear walls. *Engineering Structures*, 1995; 17(5): 344-351.
- [5] Timler PA, Kulak GL. Experimental study of steel plate shear walls. *Structural Engineering Report No. 114*, Department of Civil Engineering, University of Alberta, Edmonton, Canada, 1983.
- [6] Thorburn LJ, Kulak GL, Montgomery CJ. Analysis of steel plate walls. *Structural Engineering Report No. 107*, Department of Civil Engineering, University of Alberta, Edmonton, Canada, 1983.
- [7] Tromposch EW, Kulak GL. Cyclic and static behavior of thin steel plate shear walls. *Structural Engineering Report No. 145*, Department of Civil Engineering, University of Alberta, Edmonton, Canada, 1987.

- [8] Caccese V, Elgaaly M, Chen R. Experimental study of thin steel-plate shear walls under cyclic load. *ASCE Journal of Structural Engineering*, 1993; 119(2): 573-587.
- [9] Elgaaly M, Caccese V, Du C. Postbuckling behavior of steel-plate shear walls under cyclic loads. *ASCE Journal of Structural Engineering*, 1993; 119(2): 588-605.
- [10] Driver RG, Kulak GL, Kennedy DJL, Elwi AE. Cyclic test of four-story steel plate shear wall. *ASCE Journal of Structural Engineering*, 1998; 124(2): 112-120.
- [11] Driver RG, Kulak GL, Elwi AE, Kennedy DJL. FE and simplified models of steel plate shear wall. *ASCE Journal of Structural Engineering*, 1998; 124(2): 121-130.
- [12] Elgaaly M. Thin steel plate shear walls behavior and analysis. *Thin Walled Structures*, 1998; 32: 151-180.
- [13] Lubell AS, Prion HGL, Ventura CE, Rezai M. Unstiffened steel plate shear wall performance under cyclic loading. *ASCE Journal of Structural Engineering*, 2000; 126(4): 453-460.
- [14] Sabouri-Ghomi S, Ventura CE, Kharrazi MHK. Shear analysis and design of ductile steel plate walls. *ASCE Journal of Structural Engineering*, 2005; 131(6): 878-889.
- [15] Park HG, Kwack JH, Jeon SW, Kim WK, Choi IR. Framed steel plate wall behavior under cyclic lateral loading. *ASCE Journal of Structural Engineering*, 2007; 133(3): 378-388.

- [16] Berman J, Bruneau M. Plastic analysis and design of steel plate shear walls. *ASCE Journal of Structural Engineering*, 2003; 129(11): 1448-1456.
- [17] International Building Code, International Code Council, 2003.
- [18] Uang CMU. Establishing R (or R_w) and Cd factors for building seismic provisions. *ASCE Journal of Structural Engineering*, 1991; 117(1): 19-28.
- [19] AISC. *Seismic Provisions for Structural Steel Buildings*. 2005, Chicago, Illinois.
- [20] Miranda E, Bertero VV. Evaluation of strength reduction factors for earthquake resistant design. *Earthquake Spectra*, 1994; 10(2): 357-379.
- [21] AISC. *Specification for Structural Steel Buildings*, 2005, Chicago, Illinois.
- [22] EN 10025. *Hot rolled products of non-alloy structural steel*. CEN, European Committee for Standardization, Brussels; 1994.
- [23] Sabelli RS, Bruneau M. *Steel Plate Shear Walls*. AISC Steel Design Guide, No:20, 2007, Chicago, Illinois.
- [24] Topkaya C, Kurban OC. Natural periods of steel plate shear wall systems. *Journal of Constructional Steel Research*, Article in press, doi: 10.1016/j.jcsr.2008.03.006.
- [25] Behbahanifard MR. *Cyclic behavior of unstiffened steel plate shear walls*. Doctoral Dissertation, University of Alberta, 2003.

- [26] ANSYS Version 8.1 On-line User's Manual, 2006.
- [27] Shen C, Tanaka Y, Mizuno E, Usami T. A two-surface model for steels with yield plateau. Japan Society of Civil Engineers, Structural Engineering and Earthquake Engineering, 1992; 8(4): 179-188.
- [28] Rezai M. Seismic behavior of steel plate shear walls by shake table testing. Doctoral Dissertation, The University of British Columbia, 1999.
- [29] Krawinkler H, Seneviratna GDPK. Pros and cons of a pushover analysis of seismic performance evaluation. Engineering Structures, 1998; 20(4-6): 452-464.
- [30] Kharrazi MHK. Rational method for analysis and design of steel plate walls. Doctoral Dissertation, The University of British Columbia, 2005.
- [31] Wagner H. Flat sheet metal girders with very thin webs, Part I- General theories and assumptions. Tech. Memo. No. 604, National Advisory Committee for Aeronautics, Washington D.C., 1931.
- [32] Astaneh-Asl A. Seismic Behavior and Design of Steel Shear Walls. Steel Technical Information and Product Services Report, Structural Steel Educational Council, Moraga, CA., 2001.
- [33] FEMA 356, Prestandard and Commentary for the Seismic Rehabilitation of Buildings, Building Seismic Safety Council for the Federal Emergency Management Agency, Washington D.C., 2000.